Organic & Biomolecular Chemistry

Cite this: *Org. Biomol. Chem.*, 2011, **9**, 4367

www.rsc.org/obc

PAPER

Synthesis and physicochemical characterization of new squalenoyl amphiphilic gadolinium complexes as nanoparticle contrast agents†

Mohammad Othman,[a] Didier Desmaële,[b] Patrick Couvreur,[a] Luce Vander Elst,[c] Sophie Laurent,[c] Robert N. Muller,[c] Claudie Bourgaux,[a] Estelle Morvan,[b] Thierry Pouget,[d] Sinda Lepêtre-Mouelhi,[b] Philippe Durand[e] and Ruxandra Gref*[a]

Received 4th January 2011, Accepted 7th March 2011
DOI: 10.1039/c1ob00015b

A family of novel amphiphilic gadolinium chelates was successfully obtained by coupling the hydrophilic DOTA ligand [1,4,7,10-tetrakis(carboxymethyl)-1,4,7,10-tetraazacyclododecane] to squalenoyl moieties. Thanks to the self-assembling properties of their squalenoyl lipophilic moieties, all these derivatives were able to form, without any adjuvant, micellar or liposome-like supramolecular nanoassemblies, endowed with high relaxivities (r_1 = 15–22 mM^{-1} s^{-1} at 20 MHz and 37 °C). The remarkably high payloads of Gd^{3+} ions reached 10 to 17 wt %. Moreover, one of these derivatives interacted with human serum albumin (HSA) forming mixed micelles, which induced a remarkable increase in relaxivity. Liposome-like structures were obtained when the Gd^{3+} complex of DOTA was coupled to two squalene units. These liposomal structures were characterized by a high loading of Gd^{3+} (about 74 000 gadolinium ions per particle of 100 nm). The supramolecular architecture of these nano-objects has been investigated by electron microscopy and small-angle X-ray scattering. Squalenoylation of gadolinium derivatives offers a platform to conceive contrast agents (CAs) in mild conditions (no toxic solvents, no surfactants, no energy input). These new amphiphilic gadolinium chelates could also find potential applications in theranostics, by forming mixed systems with other squalenoylated drugs, or to delineate blood vessels owing to the interaction with HSA.

Introduction

Magnetic resonance imaging (MRI) is a widely used non-invasive imaging technique that allows investigation of opaque organisms in 3D, without employing ionizing radiation.[1–2] The images obtained by MRI are derived from the NMR signal of the protons of water molecules, where the signal intensity in a given volume is a function of both the proton relaxation times (longitudinal T_1 and transverse T_2) and concentration of water.[1] This signal intensity can be altered by the presence of contrast agents (CAs) such as gadolinium chelates (predominantly affecting T_1 relaxation) or superparamagnetic nanoparticles of iron oxide (predominantly affecting T_2 relaxation)[1–2] using specific MRI sequences. The complexes of gadolinium (Gd^{3+}) are by far the most widely used CAs for MRI in clinics, because of their highest electronic spin value ($S = 7/2$) and slow electronic relaxation rate.[3] Thus, these CAs are able to increase the contrast in MRI scans between normal and abnormal tissues and many Gd^{3+} complexes such as (Gd-DOTA) and (Gd-DTPA) [DTPA = 1,1,4,7,7-pentakis(carboxymethyl)-1,4,7-triazaheptane] were clinically approved for use in MRI. However, most CAs have insufficient relaxivities for certain applications and low tissue specificities. Moreover, a relatively high concentration of CA (0.01–0.1 mM) is necessary to produce a local alteration of the water intensity signal.[4–5] To avoid the use of high Gd^{3+} doses, which could induce toxicity in patients with renal insufficiency, more stable macrocyclic agents have been proposed.[6]

Indeed, one of the main challenges in the design of modern MRI contrast agents is to develop new systems possessing high intrinsic relaxivity in the 0.5–3 Tesla field range which is used in clinical MRI instruments.[2,7–8] This could be achieved by several strategies such as reducing the rotational motion of the Gd^{3+} complex[9] by (i) increasing the molecular size of the paramagnetic complex or (ii) by covalent or noncovalent binding to a macromolecule such as human serum albumin (HSA) or to supramolecular nanostructures.[2,10] Some of these new systems have demonstrated greater efficacy than existing clinical agents in many imaging and therapeutic applications.[5,11–14]

[a]*Univ. Paris-Sud XI, Faculté de Pharmacie, UMR CNRS 8612, 5 rue J.-B. Clément, 92296 Châtenay-Malabry Cedex, France. E-mail: ruxandra.gref@u-psud.fr; Fax: +33 1 46 83 59 46; Tel: +33 1 46 83 59 09*
[b]*Univ. Paris-Sud XI, Faculté de Pharmacie, UMR CNRS 8076 BIOCIS, 92296 Châtenay-Malabry Cedex, France*
[c]*Univ. Mons, Laboratoire de RMN et d'Imagerie Moléculaire, 19, avenue Maistriau, B-7000, Mons, Belgique*
[d]*LVMH Recherche Parfums et Cosmétiques, Département Innovation Matériaux et Technologies, 185 Avenue de Verdun, F-45804, Saint Jean de Braye, France*
[e]*CNRS, UPR 2301, (ICSN), 91198 Gif-sur-Yvette, France*
† Electronic supplementary information (ESI) available. See DOI: 10.1039/c1ob00015b

In this regard, a large number of nanosized carriers (inorganic nanocrystals, such as iron oxide, gold, nanotubes and quantum dots) as well as viruses, lipoproteins, apoferritin, hybrid nanostructures and nanogels have been loaded with Gd^{3+} chelates.[5,13–16] Particularly, nanoparticles have received considerable attention because of their good entrapment properties offering the possibility to accumulate high amounts of the CAs in organs and tissues of interest (such as tumors) either by "passive targeting" taking advantage of the enhanced permeability and retention (EPR) effect,[17] or by "active targeting" using various target-specific ligands, such as monoclonal antibodies.[18]

However, a main drawback of the existing nanoparticulate systems is their relatively low content of Gd^{3+} and their lengthy and complex preparation process. An ideal Gd^{3+} carrier would indeed (i) possess high Gd^{3+} loadings and thus high relaxivity and (ii) be able to self-aggregate in water in the absence of additional surface active agents.

To address these important goals, we have envisaged here, for the first time, the covalent coupling of Gd^{3+} chelates to squalene, a natural lipid belonging to the terpenoid family which is a precursor of the cholesterol biosynthesis. This approach is based on the exceptional properties of squalene to adopt in water a folded conformation. It has been established in our group that the linkage of nucleoside analogues to squalene, leads to amphiphilic molecules that self-organize in water to form nanoassemblies of 100–300 nm,[19] with supramolecular organisation in the hexagonal inverse phase in the case of gemcitabine–squalene (SQ-gem)[20] or in the cubic phase in the case of zalcitabine–squalene (SQ-ddC).[21] Moreover, the "squalenization" strategy has led to exceptionally high loadings of antiretroviral nucleosides zalcitabine or anticancer gemcitabine (as high as 36 or 41 wt.%, respectively).[21] Our aim here is to take advantage of the possibilities offered by the "squalenization" platform in terms of high payloads and self-assembling properties and to apply them in the field of nanoparticulate CAs.

We describe here the synthesis and characterization of new Gd^{3+} chelates–squalene derivatives (SQ-Gd^{3+}), their self-assembly in aqueous media, as well as their potential as CAs. Furthermore, one of these new SQ-Gd^{3+} complexes was used in association with SQ-gem to form SQ-gem/SQ-Gd^{3+} nanoassemblies, arising a potential application of these complexes in combination with squalenoylated nucleoside analogues in nanotheranostics for treatment and diagnosis of cancer. Interestingly, the addition of SQ-Gd^{3+} to SQ-gem, even in small amounts, induced dramatic changes in the supramolecular organization, as revealed by transmission electron microscopy (TEM) after freeze-fracture and small-angle X-ray scattering (SAXS).

Results and discussion

New amphiphilic squalene conjugates of SQ-Gd^{3+} (**2**, **3**, **4a–c**) designed to possess different structural arrangements and hydrophilic–lipophilic balances have been synthesized (Fig. 1).

At the onset of this study, we expected that the crucial coupling of the commercially available DO_3A triethyl ester (DO_3AEt) **8** with squalene could be achieved using *N*-alkylation of the secondary amino group of the cyclen **8** with *N*-squalenoyl bromoacetamide **7c** (Scheme 1). In this manner, the amide function bearing the squalenoyl chain could participate in the metal complexation and in the stabilisation of the Gd^{3+} complex. This acetamide spacer was kept for the other derivatives **3**, **4a–c** and linked to different lipophilic moieties *via* additional spacers in order to optimize the

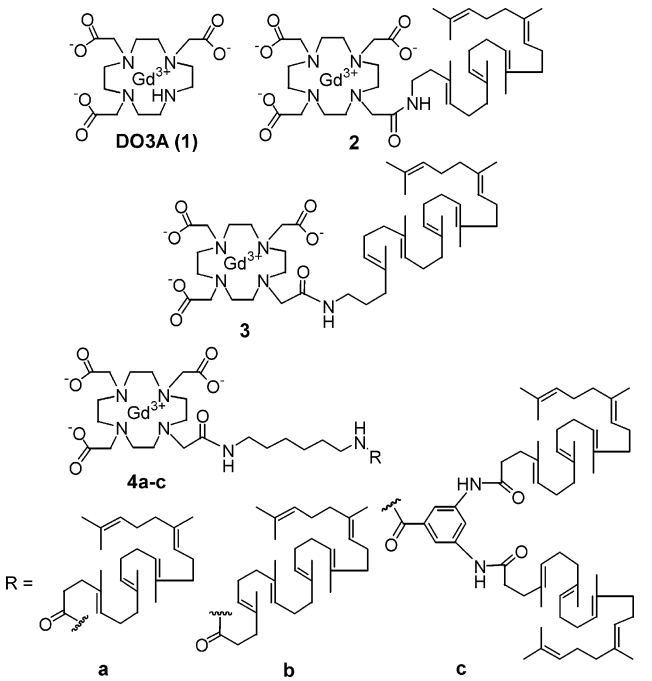

Fig. 1 Structures of DO_3A [DO_3A = 1,4,7-tris(carboxymethyl)-1,4,7,10-tetraazacyclododecane] and different synthesized squalenoyl conjugates of SQ-Gd^{3+} **2–4**.

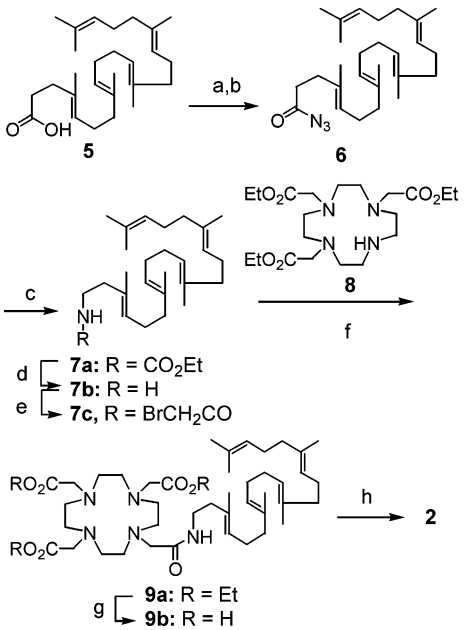

Scheme 1 Synthesis of the gadolinium complex **2**. *Reagents and conditions*: a, EtOCOCl, Et_3N, acetone, 0 °C, 30 min; b, NaN_3, H_2O, 0 °C, 90 min; c, toluene, EtOH, reflux, 15 h, 62% overall from **5**; d, KOH, EtOH, reflux, 48 h, 89%; e, $BrCH_2CO_2H$, EDCI·HCl, DMAP, CH_2Cl_2, 20 °C, 16 h, 79%; f, DO_3AEt (**8**), K_2CO_3, CH_3CN, 60 °C, 48 h, 82%; g, LiOH, MeOH, THF, H_2O, 20 °C, 15 h, 64%; h, $GdCl_3·6H_2O$, H_2O at pH = 6.5, 60 h, 20 °C, 58%.

abilities of the various structures to form nanoassemblies with high loadings of Gd^{3+}.

The synthetic route to the gadolinium complex **2** bearing a 26-carbon atom squalenoyl chain is illustrated in Scheme 1.

1,1′,2-trisnor-squalenic acid **5**, which is easily available in 4 steps from squalene,[22] was first converted into 1,1′,2,3-tetranor-squalenamine **7b**, through Curtius rearrangement of acyl azide **6** followed by basic hydrolysis of the intermediate carbamate **7a**.[23] The squalenamine **7b** was next acylated with bromoacetic acid using EDCI/DMAP as a coupling agent to give the key bromoacetamide **7c**. Alkylation of the DO_3A triethyl ester **8** with **7c** was then achieved in the presence of potassium carbonate as a base. The final unmasking of the carboxylic groups of cyclen **9a** was carried out by saponification of the three ester groups by lithium hydroxide. The gadolinium complex was then formed under pH-controlled conditions upon treatment with $GdCl_3$ at room temperature. Finally, special attention was paid to the removal of salts by sequential dialysis, C-18 reversed-phase silica gel chromatography and finally filtration through Chelex resin [24] to remove any traces of free gadolinium cations. The absence of free Gd^{3+} ions was assessed using xylenol orange indicator.[25] Thus, the gadolinium complex **2** was obtained from trisnor-squalenic acid **5** *via* an eight-step process with a 14% overall yield. Somewhat surprisingly, conjugate **2** was found to be slightly soluble in water providing micellar-type small sized nanoassemblies (Table 1). In an attempt to increase the lipophilic character of the conjugate, the gadolinium complex **3** bearing a lengthened 32-carbon squalenoyl chain was further prepared according to the same strategy (Scheme 2).

Thus, allylic alcohol **11** was obtained by aluminium isopropoxide-catalyzed ring opening [26] of the 2,3-epoxysqualene **10**,[22] and subjected to standard Johnson–Claisen rearrangement[27] to provide the predominantly (*E*) unsaturated ester **12** with a high yield. The ethyl ester **12** was then reduced by DIBAL-H to give squalenoyl alcohol **13a**. This alcohol was subsequently transformed into the corresponding phthalimide **13c** *via* the mesylate derivative **13b** followed by hydrazinolysis to give the corresponding amine **13d** through conventional Gabriel synthesis in a good overall yield.[28] Alternatively, **13c** was obtained in one step from the alcohol **13a** and phthalimide under the modified Mitsunobu reaction[29] (86% yield). Acylation of the amine **13d** with bromoacetyl bromide under Schotten–Baumann conditions delivered bromo-amide derivative **13e**, which was used to alkylate the macrocycle **8**. Subsequent saponification of the ester groups of the chelate **14** followed by complexation with $GdCl_3$ as described for **2** provided the complex **3** in a 10% overall yield from **10**.

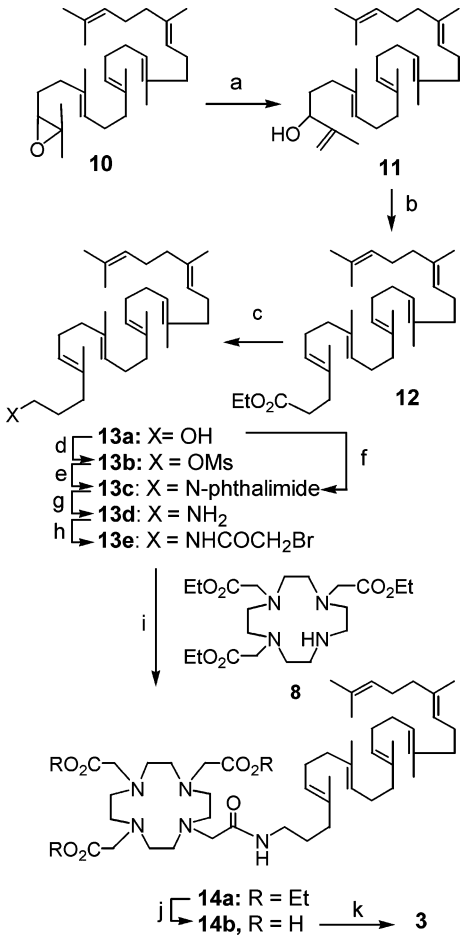

Scheme 2 Synthesis of the gadolinium complex **3**. *Reagents and conditions*: a, Al(*i*-OPr)$_3$, toluene, 110 °C, 16 h, 63%; b, $CH_3C(OCH_3)_3$, $CH_3CH_2CO_2H$ cat., 125 °C, 2 h, quantitative; c, 2.4 eq. DIBAL-H/THF, −78 °C, 5 h, 69% overall from **11**; d, CH_3SO_2Cl, Et_3N, DMAP, CH_2Cl_2, 20 °C, 16 h; e, potassium phthalimide, DMF, 70 °C, 86% overall from **13a**; f, Ph_3P, phthalimide, DIAD, anhydrous THF, 15 h, 86%; g, $H_2NNH_2{\cdot}H_2O$, EtOH, 15 h, 86%; h, $BrCH_2COBr$, CH_2Cl_2, 1 N NaOH, 0 °C, 1 h, 80%; i, DO_3AEt (**8**), K_2CO_3, CH_3CN, 60 °C, 48 h, 78%; j, LiOH, MeOH; THF; H_2O, 15 h, 20 °C, 76%; k, $GdCl_3{\cdot}6H_2O$, H_2O at pH = 6.5, 60 h, 20 °C, 68%.

The lipophilic complexes **4a–c** were designed to assess the influence of a longer spacer connecting the metal chelating moiety

Table 1 Mean hydrodynamic diameters (*d*) determined by dynamic light scattering (DLS), polydispersity index PDI, critical micelle concentration CMC at 23 °C (determined by pyrene as a fluorescent probe), and longitudinal relaxivities r_1 (mM^{-1} s^{-1}) of the five SQ-Gd^{3+} complexes (in water or HSA 4%) at 37 °C, 20 and 60 MHz. All experiments were performed in triplicate

Medium	H_2O					HSA 4%	
	d/nm	PDI	CMC/μM	r_1 20 MHz, 37 °C	r_1 60 MHz, 37 °C	r_1[a] 20 MHz, 37 °C	r_1[a] 60 MHz, 37 °C
SQ-Gd^{3+} (**2**)	9 ± 5	0.3	**9.9**	**22.2**	19.4	25.4	17.4
SQ-Gd^{3+} (**3**)	12 ± 6	0.26	**6.5**	**22.0**	20.4	31.3	27.8
SQ-Gd^{3+} (**4-a**)	21 ± 11	0.34	19.2	15.0	15.6	**36.8**	**40.7**
SQ-Gd^{3+} (**4-b**)	13 ± 7	0.29	6.8	18.9	17.8	22.8	17.8
SQ-Gd^{3+} (**4-c**)	**100 ± 20**	**0.15**	**1.3**	**22.16**	17.6	22.3	17.6

[a] For a concentration of 1 millimole of a contrast agent in HSA 4%.

to the lipophilic chain. The required building block **17b** was obtained by *N*-alkylation of cyclen derivative **8** with the known bromo acetamide **16**,[30] which was, in turn, prepared by acylation of the commercially available mono *N*-Boc-1,6-hexanediamine **15** with a high yield. Removal of the Boc-group of **17a** by treatment with trifluoroacetic acid in the presence of anisole as a *tert*-butyl cation scavenger gave compound **17b** in 83% yield from **17a** and 56% overall yield from **15** (see Scheme 3).

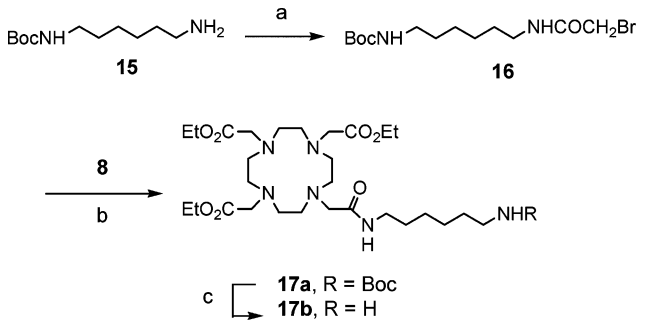

Scheme 3 The synthetic route of the key intermediate **17b**. *Reagents and conditions*: a, $BrCH_2COBr$, CH_2Cl_2, 1 N NaOH, H_2O, 45 min, 0 °C, quantitative; b, **8**, CH_3CN, K_2CO_3, 70 °C, 24 h, 67%; c, TFA, anisole, CH_2Cl_2, 4 h, 20 °C, 83%.

The syntheses of the three amphiphilic gadolinium complexes **4a–c** from the key intermediate **17b** are depicted in Scheme 4. 1,1′,2-Trisnor-squalenic acid **5** and squaleneacetic acid **19**, obtained by saponification of the corresponding ethyl ester **12**, were individually coupled to the intermediary **17b** *via* their mixed ethyl carbonic anhydride to give the squalenoyl derivatives **18a** and **20a**, respectively. Subsequent saponification of ethyl esters followed by complexation with $GdCl_3$ as described above produced complexes **4a,b** from the corresponding squalenic acid derivatives **5**, **19** in 31% and 35% overall yields, respectively.

With the aim to assemble two squalenoyl moieties on the cyclen core, we chose to organize them around the 3,5-diaminobenzoate scaffold (Scheme 4). Thus, condensation of methyl 3,5-diaminobenzoic methyl ester **21**[31] with the mixed anhydride derived from trisnor-squalenic acid **5** and ethyl chloroformate gave methyl 3,5-bis-squalenoylamido-benzoate **22a** in 85% yield. After hydrolysis of the methyl ester group, and coupling of the resulting carboxylic acid **22b** with the amine group of the protected macrocycle **17b** using EDCI·HCl as a coupling agent, the protected ligand **23a** was obtained in a 73% yield. The three ethyl ester groups of **23a** were then hydrolyzed and the gadolinium complex was formed as described above to provide the compound **4c** with 33% yield over the two step process. Thus, the SQ-Gd^{3+} **4c** was obtained from **21** *via* a five-step process with 14% overall yield.

Preparation and characterization of the SQ-Gd^{3+} complex nano-assemblies

It was shown previously that when conjugated with squalene, nucleoside analogue anticancer or antiviral drugs self-organized in water as nanoparticles,[19] forming cubic liquid crystalline phases[21] or hexagonal inverse phases.[20] The aqueous solution was found to be extended and continuous inside these structures and the amphiphilic bioconjugates adopted a particular organization, in such a way that the contact surface with water was widely amplified. This is one of the most fascinating properties of this system for MRI, as the contrast depends upon water accessibility to the Gd^{3+} ions. Moreover, squalene-based bioconjugates have potential anticancer and antiviral applications in advanced drug delivery systems.[19]

Therefore, it has been envisaged to design MRI contrast agents which could combine these advantageous characteristics with high payloads of Gd^{3+}-chelates. Additionally, the above mentioned anticancer squalene-based bioconjugates possibly will be combined with the new Gd-squalene conjugates to form composite nanoparticles with potential applications in theranostics.

Critical micelle concentration of SQ-Gd^{3+} complexes using pyrene as a fluorescent probe

The CMCs of the amphiphilic complexes were estimated by fluorescence spectroscopy using pyrene, a hydrophobic fluorescent probe that preferentially partitions into the hydrophobic core of the micelles. By this method the excitation spectrum undergoes a small shift to longer wavelengths as the probe passes from a hydrophilic to a hydrophobic environment.[32] This shift is quantified in terms of the ratio I_{336}/I_{333} of the excitation intensities at $\lambda = 333$ nm (I_{333}) for pyrene in water and $\lambda = 336$ nm (I_{336}) for pyrene in the hydrophobic environment.[33] The intensity ratios of pyrene fluorescence were plotted against the logarithm of SQ-Gd^{3+} complex concentrations in aqueous solutions. Sigmoidal curves were obtained (Fig. 4 in the ESI†). The CMC values were determined for the SQ-Gd^{3+} complex solutions from the intersection of two straight lines (the horizontal line at low concentrations with an almost constant value of the ratio I_{336}/I_{333} and a line approximating the steep upward section of the sigmoidal curve).

The synthesised novel amphiphilic Gd^{3+} complexes were shown to self-assemble in water with CMC values in the range of 19.2 to 1.3 μM (Table 1). As expected, the CMC of the CAs was found to be dependent on the carbon number of the squalene moiety. The CMC values decreased with increasing molecular weight of the squalene moieties linked to the chelates (with similar spacer), reflecting the increase in hydrophobicity of the complex (see **2** *vs.* **3** and **4a** *vs.* **4b** in Table 1). An even bigger effect was obtained when coupling two squalene moieties (see **4c** in Table 1).

These values are among the smallest reported in the literature for DOTA Gd^{3+} chelates. Indeed, CMC values of 60 μM and 0.96 μM were described for Gd^{3+} chelates linked to one and two linear C_{18} alkyl chains, respectively.[34–35] However, it should be noted that in the second case, an acyclic DTPA-based ligand with a lower affinity for Gd^{3+} was used instead of DOTA.

Noteworthily, none of the amphiphilic Gd^{3+} derivatives reported in the literature was able to self-assemble in the form of liposome-like nanostructures without the help of additional surfactants or other adjuvants which may induce potential toxicities and require complicated purification procedures.[13,35–38]

In contrast, the squalene derivatives synthesized here could self-assemble spontaneously in water in the form of micelles (compounds **2–4b**) with diameters in the range of 8 to 30 nm, or as nanoparticles for (**4c**) with a mean diameter of about 100 nm (Table 1). The size of the nano-objects increased with increasing lipophilicity of the complex particularly with two chains

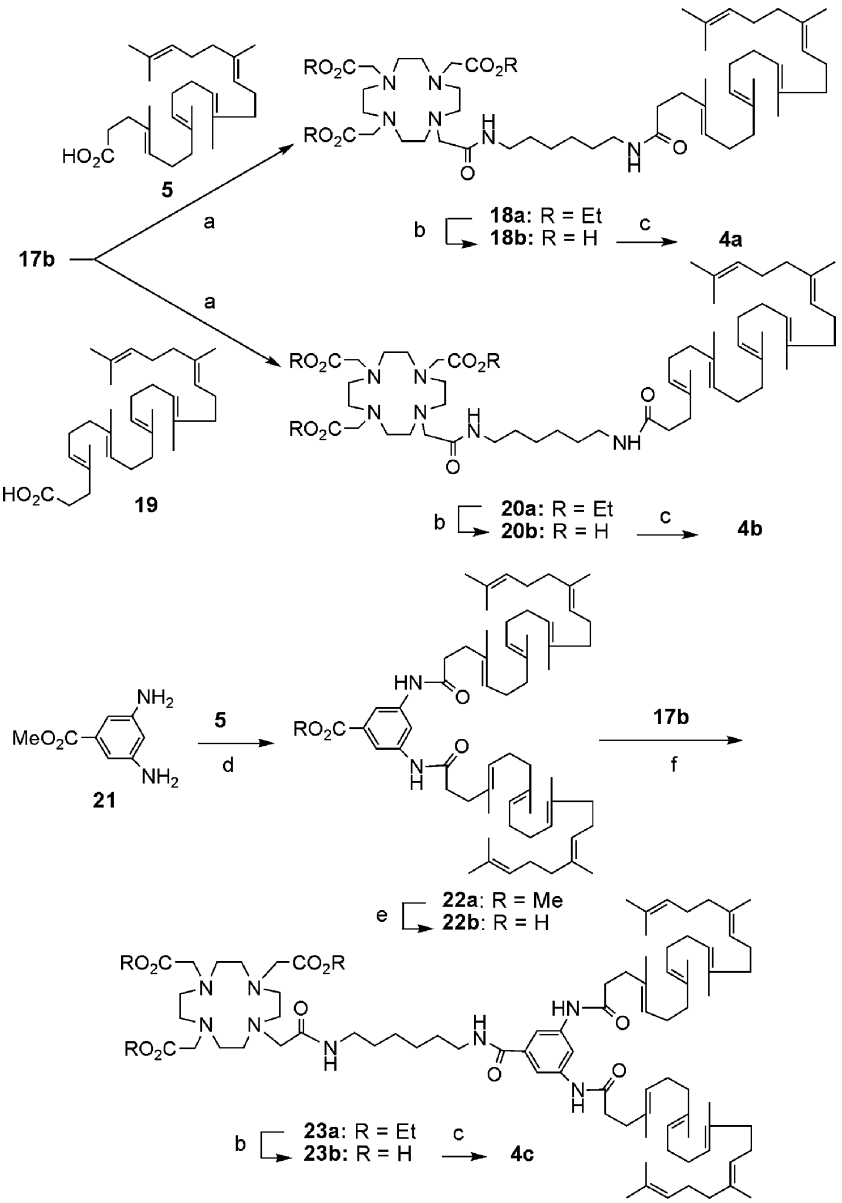

Scheme 4 Synthesis of the gadolinium complexes **4a–c**. *Reagents and conditions*: a, *i*: EtOCOCl, DMAP, Et_3N, CH_2Cl_2, 0 °C, 30 min, *ii*: **17b**, DMAP cat. 20 °C, 24 h, **18a**: 72%, **20a**: 68%. b, LiOH, MeOH; THF; H_2O, 15 h, 20 °C, **18b**: 76%, **20b**: 71%. c, $GdCl_3 \cdot 6H_2O$, H_2O, pH = 6.5, 24 h, 50 °C, **4a**: 56%, **4b**: 72%, **4c**: 33% overall yield from **23a**. d, *i*: **5**, EtOCOCl, DMAP, Et_3N, THF, 0 °C, 30 min, *ii*: **21**, 24 h, 20 °C, 85%. e, $LiOH \cdot H_2O$, EtOH, THF, reflux, 3 h, 72%. f, **17b**, EDCI·HCl, DMAP, CH_2Cl_2, 72 h, 20 °C, 73%.

of squalene (see **2–4b** *vs.* **4c** in Table 1). Interestingly, the size of all these nanoassemblies was found to be independent of the concentration of the new CAs in the range of 0.1–20 mg mL^{-1} for SQ-Gd^{3+} **2–4b**, with PDI around 0.27, and 0.1–10 mg mL^{-1} for SQ-Gd^{3+} **4c**, PDI around 0.15. This assembling process needed only the energy brought by mechanical stirring and occurred within only a few minutes. The low CMC values of these SQ-Gd^{3+} derivatives should contribute to the formation and stability of the resulting supramolecular colloidal systems in aqueous media. This could be assigned to the already reported excellent assembling capacities of squalene in water.[19,21] This clearly shows that "squalenization" is a powerful alternative to the classical approaches in CAs design, consisting of coupling alkyl chains to Gd^{3+} chelates.

Morphologies of the SQ-Gd^{3+} nanoassemblies

The morphologies of the nanoassemblies (NAs) were investigated by conventional transmission electron microscopy (TEM) and electron microscopy after freeze-fracture (FFEM). No specific architecture could be distinguished for SQ-Gd^{3+} **2**, **3**, **4a**, and **4b** suspensions, whatever their concentrations (up to 20 g L^{-1}, results not shown). However, vesicles of spherical to elliptical shape were observed in the case of the SQ-Gd^{3+} derivative **4c** (Fig. 2A and B) with conventional TEM and FFEM.

Cryogenic transmission electron microscopy (cryo-TEM)

To confirm these findings, the non destructive imaging of nanoassemblies in their suspension media (water in our case)

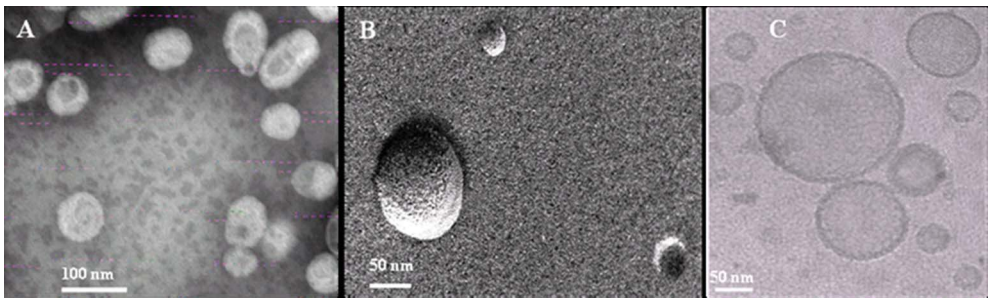

Fig. 2 Transmission electron microscopy images of SQ-Gd^{3+} complex **4c** 1% w/v in MilliQ water: (A) conventional TEM after staining with phosphotungstic acid; (B) electron microscopy after freeze-fracture FFEM; (C) cryo-TEM.

was performed using cryo-TEM. Cryo-TEM examination of **4c** revealed a homogeneous population of unilamellar liposomes with diameters of about 80–120 nm and with a shell of about 11 nm (Fig. 2). These results are consistent with size measurements by DLS and SAXS investigations, respectively. An illustration of two amphiphilic molecules that were organized in supramolecular nanoassemlies is presented in the ESI.†

Combining all the microscopic data, it was concluded that the amphiphilic chelate **4c**, which like phospholipids (has a hydrophilic head linked to a tail made of two hydrophobic chains), was able to self-organize into liposome-like NAs. To fully unravel this organization synchrotron SAXS was further used.

Small-angle X-ray scattering SAXS

SAXS was carried out on the SQ-Gd^{3+} **4c** to provide a better insight into the supramolecular organisation of the objects observed by cryo-TEM. A broad bump was observed around $q = 0.079$ Å^{-1} on the scattering curve obtained for the SQ-Gd^{3+} complex **4c** (in water at 1% w/w concentration) (Fig. 3). This pattern is consistent with the cryo-TEM experiments, suggesting the presence of unilamellar vesicles. The SAXS curve would correspond to the form factor of the liposomal membrane, with the broad bump arising from the membrane thickness. From the position of the minimum at $q \sim 0.057$ Å^{-1}, a thickness of about 110 Å can be estimated for the membrane. This value can be compared to the diameter found for micelles of SQ-Gd^{3+} **3** or **4b**. Moreover, a thickness of 48.6 Å was reported for dipalmitoylphosphatidylcholine (DPPC) membranes.[39] Since the complex **4c** with two squalenes and the chelate linked by a long spacer is bigger than DPPC, it is thus expected to form a membrane thicker than that of DPPC.

In a nut shell, both the TEM and SAXS results described above for **4c** in water indicated that SQ-Gd^{3+} complexes self-assembled into a nanostructured phase.

This system may have potential as a contrast agent for MRI for biomedical applications, since it is dispersed into nanometric particles with sizes compatible with *intravenous administration*. In addition, the stability of the **4c** dispersions was excellent, as no diameter change occurred upon more than six months of storage at 4 °C in water.

A particularly attractive feature is that the liposomal organized structures with reproducible mean diameters could be formed spontaneously without the need for time or energy consuming procedures or the help of dispersing agents, unlike in many other liposome formulation systems loaded with Gd-chelates.[40]

The principal factors involved in the formation of the self-assemblies are supposed to be primarily hydrophobic interactions, π–π stacking interactions, and steric effects on the basis of geometric considerations. Furthermore, the formation of hydrogen bonds among amide groups could also be implied in the building of these supramolecular structures.

Relaxivity of supramolecular contrast agents

The relaxivities were found to be dependent upon the structure of the Gd^{3+} derivatives (Table 1). All the SQ-Gd^{3+} complexes

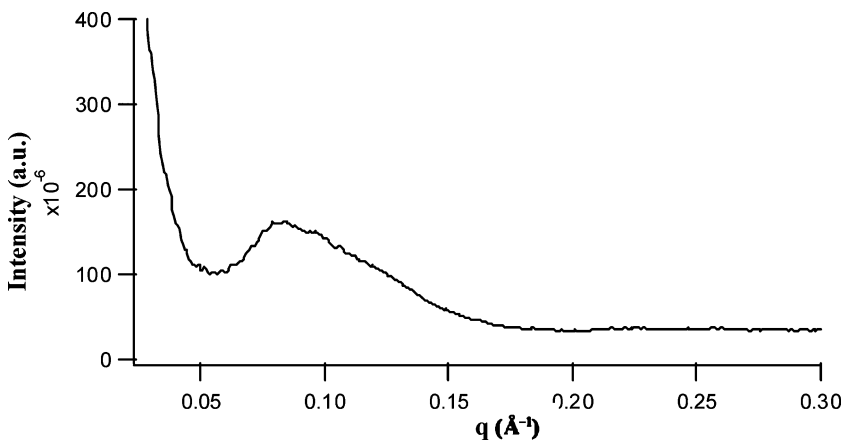

Fig. 3 SAXS pattern at 20 °C of a suspension of SQ-Gd^{3+} **4c** complex at 1% in MilliQ H_2O.

exhibited higher relaxivities (r_1 = 15–22.1 mM^{-1} s^{-1} at 20 MHz and 15.6–20.4 mM^{-1} s^{-1} at 60 MHz and 310 K) than Gd-DOTA (r_1 = 3.5 and 3.1 mM^{-1} s^{-1}, at 20 and 60 MHz and 310 K) and other commercial complexes.[41] Whatever the field, the comparison of the mean relaxivity of the four SQ-Gd^{3+} (**2–4b**) synthesized in the present study (Table 1) and characterized by similar size (micelles) highlighted the influence of the spacer between the squalene moiety and the Gd^{3+} chelate (**2**, **3** *vs.* **4a**, **4b**). The relaxivities decreased when the length of the spacer chain increased, which could be due to an increased flexibility when the rotational correlation time of the Gd^{3+} chelates decreased (Table 2). The latter effect will result in lowering of the relaxivity. At 60 MHz the comparison showed that for the same spacer the r_1 increased with the molecular weight (M_w) (**2** *vs.* **3** or **4a** *vs.* **4b** in Table 1). In the case of SQ-Gd^{3+} **4a**, the lower r_1 could result from the higher water solubility as shown by the higher CMC value of this compound.

In micellar structures, the Gd^{3+} complexes are entirely exposed to the water environment, which benefits the total measured relaxivity.[13] By comparison, approximately half of the metal centers of the complexes incorporated into the bilayer of a liposome are exposed to the exterior of the vesicle, whereas the remaining ones are directed toward the cavity, which could limit the relaxivity.[5,13,42] Surprisingly, very similar relaxivities were obtained at 20 MHz for micellar SQ-Gd^{3+} (**2** and **3**) and for the liposomal-like structures (**4c**) (Table 1). Thus, there is no obvious correlation of the M_w increase of the various Gd^{3+} chelates with their relaxivities, as was the case with dendrimeric Gd^{3+} chelates, where the relaxivity increased with increasing the M_w.[43]

It was previously established that the presence of an unsaturated carbon–carbon bond in the alkyl chain of an amphiphilic Gd^{3+} complex induced an increase in its mobility and its water exchange rate. This may explain the better efficacy for MRI in liposomal formulations.[42] The two squalene units of the SQ-Gd^{3+} **4c** contain 10 unsaturated carbon–carbon bonds and 3 bonds in the aromatic benzoic scaffold. It should be noted that aliphatic CH groups and aromatic CH groups make different contributions to the overall molecular hydrophobicity, according to Hansch's π parameters.[44] Therefore, the aliphatic and aromatic unsaturated bonds could contribute differently to the hydrophobicity and subsequently to the rigidity of the complex.

The measurement of water proton relaxation rate over an extended range of magnetic field strengths (0.02–400 MHz in the NMRD experiment) is a complementary method for the complete characterization of a paramagnetic complex. The relaxivity measurements were performed on samples at concentrations higher than the CMC. Under these conditions, the contribution of monomeric species is assumed to be negligible, and only aggregates are responsible for the measured relaxivity values. The resulting plot of r_1 *versus* the proton Larmor frequency, NMRD profiles, for **2–4c** are presented in Fig. 4. The profiles show that these complexes possess high relaxivity values at all fields, with a typical peak at higher frequencies centered at 20–60 MHz, except for **4a** which has the lowest critical micelle concentration. The NMRD profiles of the micelles are characteristic of slowly tumbling molecules, caused by an increase in the rotational correlation times (τ_R) as compared with low molecular weight Gd^{3+} complexes.[34] The relaxivity values were found to be similar to those reported for other Gd^{3+} complexes bound to macromolecules.[16,43] Moreover, the amount of Gd^{3+} complexes per particle was high; this extremely enhanced the total relaxivity per contrast agent particle. In all SQ-Gd^{3+} supramolecuar structures, the Gd^{3+} ion represented between 10 and 17 wt.% of the particle according to the M_w. The calculated numbers of SQ-Gd^{3+} per micelle (**2–4b**) were about 120–540 molecules (see the ESI†); however, for the liposome-like structure **4c** it was found to be about 74 000 molecules per particle (see the ESI†) which is 1.85 times greater than the number reported in the literature (40 000 per liposome).[40,45] The rotational correlation time was strictly related to the size and to the rigidity of the investigated system. Both the global (τ_{Rg}) and the local (τ_{Rl}) rotational correlation times could be influenced by the length and by the hydrophobicity of the side chain in the amphiphilic Gd^{3+} complex. The water residence time (τ_M) was estimated by O-17 relaxometry for complexes **2** and **4b**. The τ_M values were found to be close (152 ± 44 ns for **2** and 181 ± 77 ns for **4b** at 310 K) (see the ESI†). These values were used to fix the variation range of τ_M for all the complexes.

Theoretical fittings of the relaxometric data were performed using the classical outer sphere and inner sphere theories and the Lipari–Szabo approach. The results (Table 2) show that complexes **2**, **3** and **4b** have quite similar profiles and do not experience significant local mobility (s^2 = 0.88–1). The global τ_R were similar for the three complexes, in agreement with their comparable micellar size. However, they were lower than that expected from the hydrodynamic diameters and corresponded to diameter values close to 2.3 nm. The relaxometric profile of complex **4a**, which was found to be characterized by the larger CMC and by a bigger diameter, was clearly different from the former ones, more particularly between 10 and 100 MHz. It appeared that the fitting

Table 2 Values of the global rotational correlation time (τ_{Rg}), the local rotational correlation time (τ_{Rl}), the water residence time (τ_M), the electronic relaxation time at zero field (τ_{SO}), the time modulating the electronic relaxation time (τ_V) and of s^2 obtained from the theoretical fitting of the relaxometric data[a]

SQ-Gd^{3+}	**2**	**3**	**4a**	**4b**	**4c**
τ_{Rg}/ps	881 ± 14	890 ± 20	558 ± 0.1	771 ± 23	956 ± 24
τ_{Rl}/ps	(495 ± 54)[b]	(500 ± 39)[b]	(30.3 ± 0.04)[b]	146 ± 49	(498 ± 13)[b]
τ_M/ns	200 ± 6	206 ± 9	105 ± 0.7	103 ± 28	207 ± 11
τ_{SO}/ps	190 ± 2	190 ± 0.8	200 ± 0.1	190 ± 0.3	200 ± 0.1
τ_V/ps	50 ± 0.06	50 ± 0.05	50 ± 0.06	50 ± 0.08	50 ± 0.04
s^2	1 ± 0.03	1 ± 0.02	1 ± 0.003	0.88 ± 0.03	1 ± 0.001

[a] The following parameters were fixed: d, the distance of closest approach of the outer sphere water proton nuclei was set to 0.36 nm; r, the distance between Gd^{3+} ion and the protons of the coordinated water molecule of the inner sphere was fixed to 0.31 nm; D, the diffusion coefficient was set to 3.3×10^{-9} m^2 s^{-1}, τ_M was allowed to vary from 100 to 250 ns. [b] These values have no real meaning since s^2 was found to be close to 1.

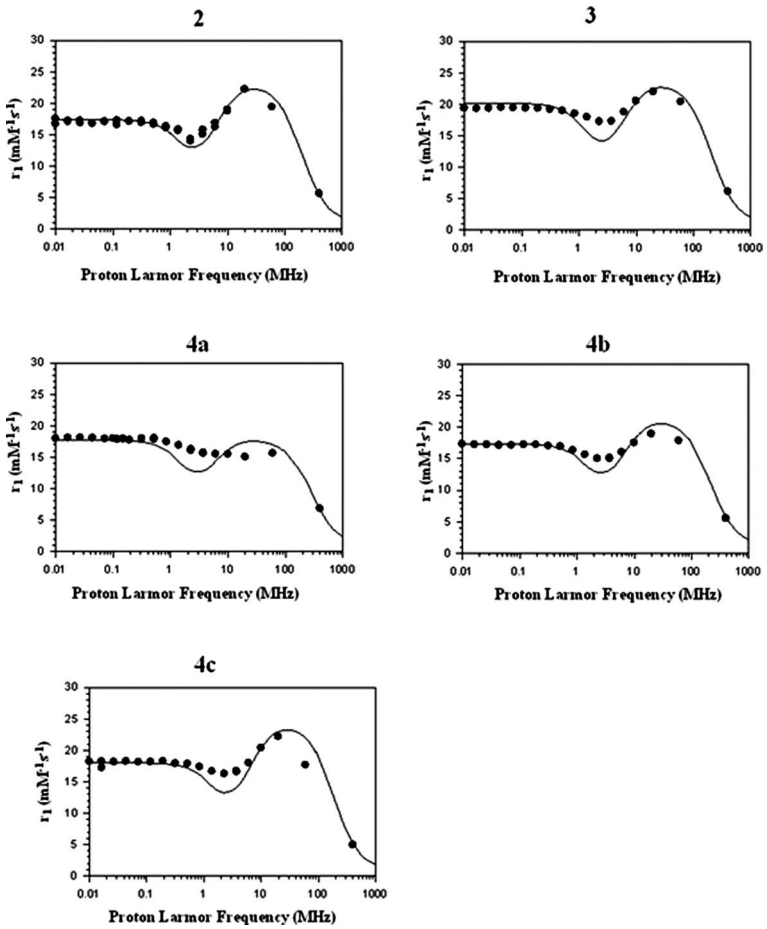

Fig. 4 ^{1}H NMRD relaxivity profiles of five squalene based Gd^{3+}complexes in water at 310 K. The lines correspond to the theoretical fitting of the data points.

was not adequate, probably because of the coexistence of several structures and therefore several correlation times, it seems that this complex did not form quite well defined micelles. However, unfortunately, the DLS data of complex **4a** were not reproducible due to the presence of several populations; the polydispersity of this derivative was too large to ensure a good measurement. For the last complex **4c**, the fitting was performed assuming that all the Gd^{3+} ions contributed to the relaxivity. In other words, it was assumed that the exchange rate of water through the membrane was not limiting the relaxation rate arising from the complexes located inside the liposome. The data obtained from the fitting agreed with some flexibility of the complexes since τ_{Rg} was lower than 1 ns.

The relaxivities obtained here are among the highest values reported in the literature for CAs that are capable of presenting self-organization. For instance, the reported relaxivity of a (Gd-DOTA·Chol) cholesterol derivative was 4.42 mM^{-1} s^{-1} at 25 °C and 20 MHz, which was in the same order of values as the clinically used Dotarem (5.25 mM^{-1} s^{-1} at 25 °C and 20 MHz), thus indicating that Gd-DOTA·Chol was unable to self-aggregate.[46]

The amphiphilic Gd-DOTA coupled to C_{18} chains had an r_1 of 17 mM^{-1} s^{-1} at 60 MHz and 25 °C,[34] which is in the same order of magnitude as the SQ-Gd^{3+} (**2–4c**) complexes (Table 1). Comparable relaxivities as for **4c** were reported for DTPA-Gd^{3+} complexes coupled to two C_{18} chains (r_1 21 mM^{-1} s^{-1} at 20 MHz, 25 °C).[35] The r_1 of the complex **4c** (M_w = 1556.21 g mol^{-1}) was found to be 1.5 times greater than that reported by Pierre *et al.*[43] with a dendrimeric Gd^{3+} chelate of similar molecular weight (M_w = 1576 g mol^{-1}), r_1 = 14.3 mM^{-1} s^{-1} at 20 MHz, and 25 °C.

Interaction of SQ-Gd^{3+} complexes with human serum albumin HSA

HSA is the most abundant plasma protein (concentration of about 4%), involved in several physiological functions such as homeostasis, metabolism, protection and also binding and transport of a number of endo- and exogenous substrates with a relatively high affinity.[47,48]

Two major binding sites can be distinguished, according to the Sudlow classification scheme.[47] The Sudlow site II is a hydrophobic pocket which binds small aromatic carboxylic acids, like L-tryptophan or ibuprofen, while the Sudlow site I is reported as a large and flexible region[47] able to bind a wide diversity of ligands such as salicylate, warfarin or bilirubin.[48] Long-chain fatty acids (C_{16}, C_{18}, and C_{20}) were bound in about six sites, the strongest of them are in different domains: loops 8–9, 6, 3.[47] Binding of a CA to HSA can be advantageous to retain the agent in the blood pool and increase its relaxivity in plasma.[49] Thus, some conjugates

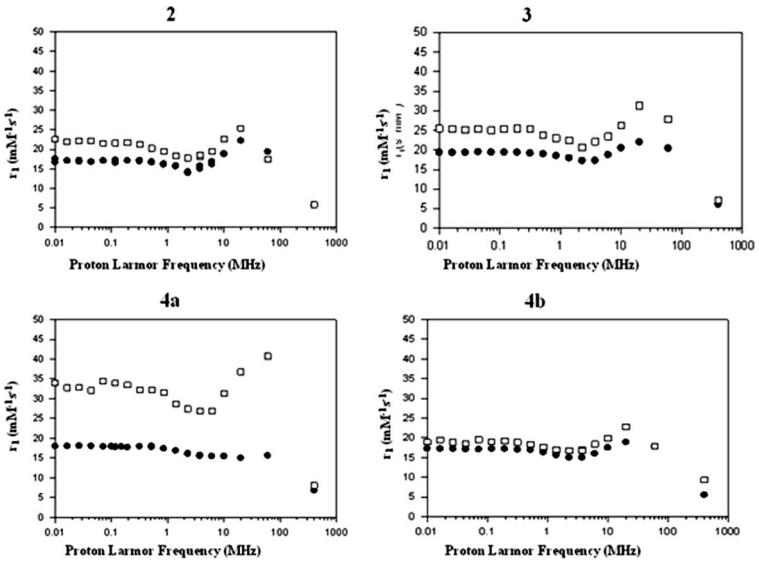

Fig. 5 Comparison of the ^{1}H NMRD relaxivity profiles of the four squalene-based Gd^{3+} complexes **2**, **3**, **4a** and **4b** in ● water and □ HSA 4% solutions at 310 K. The concentrations of **2**, **3**, **4a** and **4b** were equal to 1 mM.

have been used to delineate the blood vessels in which they were confined.[2,12]

The interaction of a low molecular weight Gd^{3+} complex with HSA increases its rotational correlation time τ_R and subsequently enhances its relaxivity. The resulting relaxivity increase depends on the relative amounts of free and bound contrast agents, and therefore on the strength of the interaction and on the intensity of the magnetic field. This phenomenon was used to evaluate the non-covalent interaction of SQ-Gd^{3+} complexes with HSA (Fig. 5).

The presence of HSA did not significantly change the shape and the values of the relaxometric profiles of **2**, **3** and **4b**. The slight r_1 increase could be related to the enhanced viscosity of the HSA solution. In the presence of HSA, significant relaxation enhancement was observed with SQ-Gd^{3+} **4a**, showing an obvious interaction of this complex with HSA. The difference between the behaviour of this complex as compared to the three others can probably be explained either by (i) the presence of non-aggregated complex in water solution which is able to interact with HSA, thus inducing an increase of the relaxation rate or (ii) by the breakdown of the micellar structure in the presence of HSA with subsequent interaction of the complex with HSA. The relaxivity of the most hydrophobic compound, **4c**, was unchanged at 20 and 60 MHz (at 20 MHz r_1 = 22.16 mM^{-1} s^{-1} in water and 22.3 mM^{-1} s^{-1} in HSA; at 60 MHz, r_1 = 17.6 mM^{-1} s^{-1} in water and 17.6 mM^{-1} s^{-1} in HSA). This is probably due to the supramolecular organisation of **4c** which is too stable to interact with HSA. Indeed, upon mixing **4c** with a HSA 4 wt.% solution, the mean diameter of the nanostructures was not modified as revealed by dynamic light scattering (DLS).

The mixed micelles of HSA and SQ-Gd^{3+} **4a** (0.11 mM) presented a relaxivity r_1 of 43.1 mM^{-1} s^{-1} at 20 MHz. This r_1 value was comparable to the one reported for Ms-325,[50] which was designed as a CA for imaging the blood pool using HSA as the targeted binding molecule.[2] As the SQ-Gd^{3+} **4a** concentration increased from 0.11 to 2.75 mM, the apparent r_1 decreased from 43.1 to 34.4 mM^{-1} s^{-1}. These data agree with a larger amount of **4a** complex bound to HSA at lower concentration and might suggest that the interaction with HSA could occur through multiple non-identical binding sites, giving rise to variable degrees of relaxation enhancement as for Ms-325.[2]

Theranostic

We have further investigated the possibility to associate in the same nanoparticle structure, the efficient anticancer bioconjugate SQ-gem [19,20] with the newly synthesized CA SQ-Gd^{3+} **2**.

It was found that the addition of SQ-Gd^{3+} **2** to SQ-gem, even in small amounts, dramatically changed the nanoparticle supramolecular organization, as shown in FFEM images (Fig. 6B). Indeed, whereas the pure SQ-gem NAs presented close-packed tube-like structures (inverse hexagonal phase) (Fig. 6A), as already reported,[21] SQ-gem/SQ-Gd^{3+} **2** NAs were compact with a regular inner structure, suggesting an inverted bicontinuous cubic phase.

The structure of the SQ-gem/SQ-Gd^{3+} **2** nanocomposites was further investigated by small-angle X-ray scattering SAXS. Their SAXS profile showed a broad band in which peaks at 0.086, 0.1034, 0.144, and 0.166 $Å^{-1}$ could be resolved (Fig. 6C). This set of Bragg reflections is consistent with a cubic lattice of space group *Pn3m* having a lattice parameter of ~100 Å. The calculated (110), (111), (200), (211), (220) and (221) Bragg reflections of this structure, spaced in the ratios $\sqrt{2}$, $\sqrt{3}$, 2, $\sqrt{6}$, $\sqrt{8}$ and 3, should be observed at 0.086, 0.1053, 0.1216, 0.149, 0.172 and 0.1824 $Å^{-1}$. The reflection at 0.1216 $Å^{-1}$ cannot be experimentally resolved, probably because of the width of overlapping peaks. This lack of resolution could result from the small coherence length of the lattice and/or from internal disorder. This SQ-gem/SQ-Gd^{3+} inverse bicontinuous cubic phase could be described as a bilayer whose mid-plane lies on the D (Diamond) periodic minimal surface.[51,52] Note that the inverse bicontinuous phase is intermediate between the lamellar and the inverse hexagonal phases in the usual sequence of phases observed when the spontaneous monolayer curvature becomes increasingly negative.

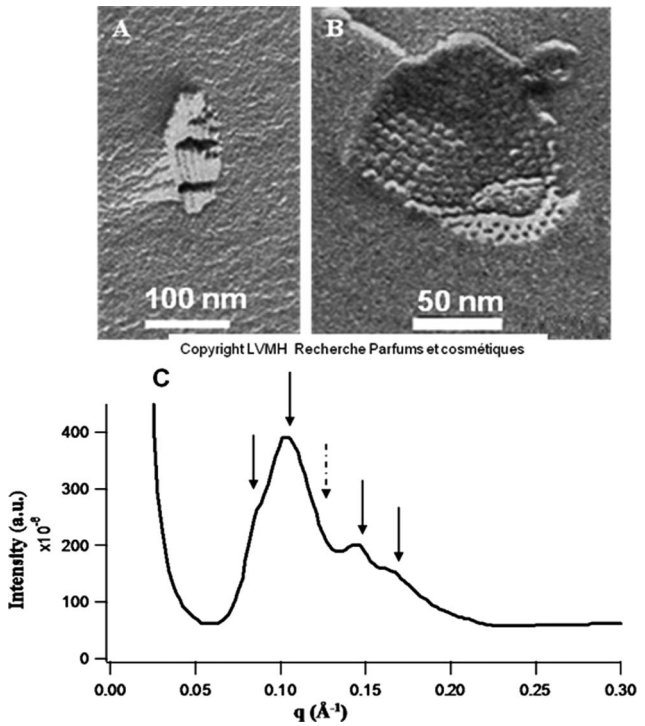

Fig. 6 Transmission electron microscopy after freeze fracture images of: (A) nanoparticles of gemcitabine-squalene (SQ-gem) 4 mg mL^{-1}; (B) the composite nanoparticles of SQ-gem/SQ-Gd^{3+} complex **2** (4/0.5 mg mL^{-1}); (C) small-angle X-ray diffraction pattern of SQ-gem/SQ-Gd^{3+} **2** nanocomposites in excess water shown on a linear scale, arrows denote Bragg reflections of the *Pn3m* cubic structure.

The above observations support the assumption that SQ-gem and SQ-Gd^{3+} **2** associated very effectively together in water to form the SQ-gem/SQ-Gd^{3+} **2** nanocomposites, presumably through strong hydrophobic interactions between their respective SQ moieties. Thus, the SQ-gem/SQ-Gd^{3+} **2** nanocomposites were characterized by satisfying payloads of Gd^{3+} complex of 22.5 ± 2.8% (weight Gd^{3+} complex **2**/weight SQ-gem) as determined by the Evans method, and consequently by a high relaxivity r_1 of 20.1 mM^{-1} s^{-1} (at 20 MHz and 37 °C), which is comparable to that of SQ-Gd^{3+} **2** alone. A particularly attractive feature is that an organized structure with high hydrophilic surface-to-volume ratio formed spontaneously, allowing large water accessibility to the Gd^{3+} ions.

Cytotoxicity assay on MIA PaCa-2 cells

Additionally, cytotoxicity assays were carried out on aggressive human pancreatic cancer cells (MIA PaCa-2). Gemcitabine displayed cytotoxicity on this cell line with a 50% inhibitory concentration (IC_{50}) value of 11.8 ± 2.5 μM. This value was lower in the case of SQ-gem (IC_{50} = 8.9 ± 2.1 μM) and SQ-gem/SQ-Gd^{3+} **2** (IC_{50} = 7.1 ± 1.6 μM). Notably, the SQ-Gd^{3+} **2** alone at similar concentrations present in the SQ-gem/SQ-Gd^{3+} **2** composite nanoparticles did not show cytotoxicity on these cells.

In conclusion, the association of the new SQ-Gd^{3+} **2** CA to SQ-gem leads to the formation of composite nanoassemblies with (i) different inner structure compared to the starting material; (ii) good relaxivities and (iii) unperturbed cytotoxic capabilities.

Conclusions

A class of new amphiphilic paramagnetic CAs with high relaxivities has been synthesized and characterized. All the CAs were able to form supramolecular assemblies, with high payloads of Gd^{3+} ions (up to 74 000 Gd^{3+} complex per particle). Furthermore, one of these CAs could bind to HSA resulting in a remarkable increase in the relaxivity.

Thus, squalenoylation of Gd^{3+} derivatives offers a platform to conceive CAs with a greater degree of relaxivity efficacy. For the first time, unilamellar liposome-like structures with homogeneous size could be formed spontaneously. Furthermore, the use of other components such as phospholipids was unnecessary in this case.

These new Gd^{3+} derivatives could find different potential applications according to their molecular structure. Therefore, the chelates coupled with one squalenoyl moiety interacted with HSA and presented high relaxivities, whereas the one coupled with two squalenoyl moieties did not. These compounds may also find application in theranostics for personalized and optimized treatments for patients, by forming mixed systems with anticancer prodrugs.

Experimental methods and materials

Materials

All the chemicals used were of analytical grade and were used without further purification. Gemcitabine hydrochloride was purchased from Sequoia Research Products Ltd. (UK). 1-Ethyl-3-(3-dimethylaminopropyl)carbodiimide hydrochloride (EDCI·HCl), aluminium isopropoxide, bromoacetic acid, diisobutylaluminum hydride solution 1.0 M in cyclohexane (DIBAL-H), diisopropyl azodicarboxylate (DIAD), 4-(dimethylamino)pyridine (DMAP), ethyl chloroformate, gadolinium(III) chloride hexahydrate, *N*-Boc-1,6-diaminohexane, phthalimide, pyrene, anisol, hydrazine monohydrate, xylenol orange sodium salt indicator for metal titration and human serum albumin (HSA, product no. A-1653, Fraction V powder 96–99%) were purchased from Sigma-Aldrich. Triethyl orthoacetate and methyl 3,5-diaminobenzoate were purchased from Alfa Aesar. Propionic acid was from Lancaster. Chelating resin: Chelex 100 sodium form was from Bio-Rad Laboratories. Amberlite® IR 120 H resin, bromoacetyl bromide, potassium sodium tartrate tetrahydrate, potassium phthalimide, *tert*-butanol, trifluoroacetic acid (TFA) and triphenylphosphine (Ph_3P) were purchased from Acros Organics. Lithium hydroxide monohydrate and methanesulfonyl chloride (MsCl) were purchased from Merck, potassium carbonate was from Carlo Erba. 1,4,7,10-Tetraazacyclododecane-1,4,7-triacetic acid triethyl ester (DO_3AEt) was purchased from Chematec France. Dialysis membrane Spectra/Por® cellulose ester (CE) (molecular weight cut-off, MWCO = 500 Dalton) was purchased from Spectrum Laboratories Inc. *via* Interchim France. WATER (17O, 35–40%), OLM- 782-40-1 was obtained from Cambridge Isotope Laboratories, Inc. MA, USA. 4-(N)-trisnor-squalenoyl gemcitabine (SQ-gem) was synthesized as previously described.[19]

Methods

The ^1H and ^{13}C NMR spectra were recorded on Bruker Avance 300 (300 MHz and 75 MHz, for ^1H and ^{13}C, respectively) or

Bruker Avance 400 (400 MHz and 100 MHz, for ^1H and ^{13}C, respectively) spectrometers. Shifts of ^1H and ^{13}C NMR spectra were calibrated against the solvent residual isotopic peak as internal reference. Recognition of methyl, methylene, methine, and quaternary carbon nuclei in ^{13}C NMR spectra rests on the *J*-modulated spin-echo sequence. IR spectra were obtained as solid or neat liquid on a Fourier Transform Bruker Vector 22 spectrometer. Only significant absorptions were listed. Low resolution mass spectra (MS) were recorded using electrospray ionization (ESI) conditions in a positive-ion or a negative-ion mode on an (Esquire LC Bruker spectrometer; USA). High-resolution mass spectra (HRMS) were recorded using either ESI or MALDI-TOF ionization on a (ESI/TOF; LCT, Waters; USA) mass spectrometer or a (Voyager-DE STR, Applied Biosystems; USA) mass spectrometer, respectively, at the "Service de Spectrométrie de Masse – IMAGIF/ICSN – CNRS, Gif-sur-Yvette – France". Elemental analyses were performed by the "Service de microanalyse du Centre d'Etudes Pharmaceutiques" (Châtenay-Malabry, France) with a Perkin Elmer 2400 analyzer. The gadolinium content in the complexes was determined at the "Service Central d'Analyse du CNRS (Solaize, France)" by inductively coupled plasma atomic emission spectroscopy (ICP-AES) on an ICP-AES – JOBIN YVON spectrometer. All reactions were performed under nitrogen atmosphere unless stated otherwise. Pyridine, triethylamine, toluene, acetonitrile, dichloromethane and *N*,*N*-dimethylformamide (DMF) were distilled from calcium hydride and stored over 4 Å molecular sieves. Diethyl ether and tetrahydrofuran (THF) were distilled from sodium benzophenone ketyl. Ethyl acetate, cyclohexane, and other organic solvents used in chromatography were distilled before using. Analytical thin-layer chromatography was performed on Merck silica gel 60 F_{254} glass precoated plates (0.25 mm layer) or RP-18 (F_{254}, Merck) plates. TLC plates were viewed under UV light (254 nm) and visualized with I_2, Kägi–Misher or Draggendorf reagents. Column chromatography was performed on Merck silica gel 60 (230–400 mesh ASTM). A C-18 reversed-phase 100 silica gel was used for column chromatography of the Gd^{3+} complexes (particle size 40–63 μm, surface coverage 17–18%, Fluka).

Ethyl-(3,7,12,16,20-pentamethylhenicosa-3,7,11,15,19-pentaen-1-yl)-carbamate (7a). To an ice-cooled stirred solution of 1,1′,2-trisnor-squalenic acid (**5**) (1.0 g, 2.5 mmol) in anhydrous acetone (10 mL) was added distilled triethylamine Et_3N (0.305 g, 3 mmol) followed by ethyl chloroformate (0.325 g, 3 mmol). The reaction mixture was stirred at 0 °C for 30 min, then a solution of sodium azide (0.65 g, 10 mmol) in distilled water (3 mL) was added dropwise over 5 min. The reaction mixture was further stirred at 0 °C for 90 min, then water (10 mL) was added. The mixture was extracted with toluene (5 × 20 mL). The combined organic phases were dried over $MgSO_4$, filtered and concentrated under reduced pressure (0.5 Torr) while keeping the bath temperature below 40 °C to give the crude acyl azide **6** (1.15 g quantitative) as a colorless oil which was used directly in the next step without further purification. IR (neat, cm^{-1}) ν = 2916, 2135, 1720, 1444.

The crude acyl azide **6** (2.05 g, 5.12 mmol) in a mixture of toluene/anhydrous ethanol (13 mL, 10/3 v/v) was heated under reflux for 15 h. After cooling, the reaction was concentrated under reduced pressure and the residue was purified by column chromatography on silica gel, eluting with (cyclohexane/EtOAc, 4/1 v/v) to give the carbamate **7a** as a pale yellow oil (1.41 g, 62% overall yield from **5**). IR (neat, cm^{-1}) ν = 2915, 1708, 1511, 1445, 1381, 1250; ^1H NMR (300 MHz, $CDCl_3$) δ: 5.20–5.05 (m, 5 H, *H*C═C), 4.58 (broad s, 1 H, NH), 4.09 (q, *J* = 6.9 Hz, 2 H, OC*H*$_2$CH$_3$), 3.24 (m, 2 H, CONC*H*$_2$), 2.14 (t, *J* = 6.9 Hz, 2 H, CONCH$_2$C*H*$_2$), 2.15–1.90 (m, 16 H, ═CC*H*$_2$C*H*$_2$), 1.67 (s, 3 H, (C*H*$_3$)$_2$C═), 1.60 (s, 15 H, ═C(C*H*$_3$)CH$_2$), 1.23 (t, *J* = 6.9 Hz, 3 H, OCH$_2$C*H*$_3$); ^{13}C NMR (75 MHz, $CDCl_3$) δ: 156.5 (*C*ONH), 135.1 (C), 134.8 (C), 134.7 (C), 131.6 (C), 131.2 (C), 127.0 (CH), 124.6 (CH), 124.4 (CH), 124.2 (2 CH), 60.6 (CH$_2$), 39.7 (2 CH$_2$), 39.6 (2 CH$_2$), 38.6 (CH$_2$), 28.1 (2 CH$_2$), 26.7 (CH$_2$), 26.6 (CH$_2$), 26.5 (CH$_2$), 25.7 (CH$_3$), 17.5 (CH$_3$), 16.0 (CH$_3$), 15.8 (2 CH$_3$), 15.5 (CH$_3$), 14.6 (CH$_3$); MS (APCI$^+$) *m*/*z* (%) = 444.4 (100) [M+H]$^+$. Anal. Calcd for $C_{29}H_{49}NO_2 \cdot H_2O$: C, 75.44, H, 11.13, N, 3.03. Found: C, 75.54, H, 10.8, N 3.03.

3,7,12,16,20-Pentamethyl-heneicosa-3,7,11,15,19-pentaenyl-amine (7b). The carbamate **7a** (1.02 g, 2.31 mmol) was treated with 1 M ethanolic potassium hydroxide (30 mL, 30 mmol). The mixture was heated under reflux for 48 h. After cooling the reaction mixture was concentrated under reduced pressure. The residue was taken up in distilled water (10 mL) and extracted by diethyl ether (4 × 25 mL). The combined organic extracts were dried over $MgSO_4$, filtered and concentrated *in vacuo*. The residue was purified by flash chromatography on silica gel (cyclohexane/EtOAc/Et_3N, 20/10/0.1 v/v/v, EtOAc/Et_3N, 10/0.05 and EtOAc/MeOH/Et_3N 9/1/0.05) to provide tetranor-squalenamine **7b** as a light yellow oil (0.77 g, 89% yield). IR (neat, cm^{-1}) ν = 2963, 2915, 2852, 1569, 1441, 1381; ^1H NMR (300 MHz, CD_3OD) δ: 5.28–5.04 (m, 5 H, *H*C═C), 2.76 (t, *J* = 7.1 Hz, 2 H, NC*H*$_2$), 2.20–1.95 (m, 18 H), 1.70 (s, 3 H, C*H*$_3$), 1.65 (s, 3 H, C*H*$_3$), 1.63 (s, 12 H, 4 C*H*$_3$); ^{13}C NMR (75 MHz, CD_3OD) δ: 136.1 (C), 136.0 (C), 135.9 (C), 132.9 (C), 132.1 (C), 128.1 (CH), 125.7 (CH), 125.6 (CH), 125.5 (2 CH), 42.7 (CH$_2$), 40.9 (2 CH$_2$), 40.8 (CH$_2$), 40.1 (CH$_2$), 29.3 (2 CH$_2$), 27.9 (CH$_2$), 27.7 (CH$_2$), 27.6 (CH$_2$), 26.0 (CH$_3$), 17.8 (CH$_3$), 16.3 (3 CH$_3$), 15.9 (CH$_3$); MS (ESI$^+$) *m*/*z* (%) = 372.6 (100) [M+H]$^+$; Anal. Calcd for $C_{26}H_{45}N$. 0.7 H_2O: C, 81.4, H, 12.17, N, 3.65. Found: C, 81.59, H, 11.67, N, 3.61.

2-Bromo-*N*-(3,7,12,16,20-pentamethyl-henicosa-3,7,11,15,19-pentaenyl)-acetamide (7c). To a stirred solution (0.62 g, 1.66 mmol) of a tetranor-squalenamine **7b** in CH_2Cl_2 (4 mL), was added bromoacetic acid (0.35 g, 2.5 mmol), 1-ethyl-3-(3-dimethylaminopropyl)carbodiimide-hydrochloride (EDCI·HCl) (0.32 g, 1.67 mmol), DMAP (0.032 g, 0.26 mmol) and lithium bromide (0.30 g, 3.5 mmol, added to minimize bromine/chlorine exchange due to EDCI·HCl). After being stirred at 20 °C for 16 h, water (10 mL) was added and the reaction mixture was extracted with CH_2Cl_2 (3 × 20 mL). The combined organic phases were dried over $MgSO_4$, filtered and concentrated *in vacuo*. The residue was purified by flash chromatography on silica gel (cyclohexane/EtOAc, 2/1 v/v) to yield bromoacetamide **7c** (0.645 g, 79%) as a light yellow oil. IR (neat, cm^{-1}) ν = 2925, 2852, 1653, 1541, 1445, 1382, 1211; ^1H NMR (300 MHz, $CDCl_3$) δ: 6.51 (broad s, 1 H, N*H*CO), 5.25 (t, *J* = 6.6 Hz, 1 H, *H*C═C), 5.20–5.00 (m, 4 H, *H*C═C), 3.86 (s, 2 H, BrC*H*$_2$), 3.40–3.30 (m, 2 H, OCNHCH$_2$), 2.20 (t, *J* = 6.6 Hz, 2 H, OCNHCH$_2$C*H*$_2$), 2.20–1.90 (m, 16 H, ═CC*H*$_2$C*H*$_2$), 1.67 (s, 3 H), 1.62 (s, 3 H, (C*H*$_3$)$_2$C═), 1.59 (s, 12 H, ═C(C*H*$_3$)CH$_2$); ^{13}C NMR (75 MHz, $CDCl_3$) δ:

165.2 (C), 135.2 (C), 135.0 (C), 134.9 (C), 131.3 (2 C), 127.9 (CH), 124.6 (CH), 124.5 (CH), 124.4 (CH), 124.3 (CH), 39.8 (2 CH_2), 39.7 (CH_2), 38.8 (CH_2), 37.8 (CH_2), 29.5 (CH_2), 28.4 (2 CH_2), 27.0 (CH_2), 26.9 (CH_2), 26.7 (2 CH_2), 25.8 (CH_3), 17.8 (CH_3), 16.1 (3 CH_3), 15.6 (CH_3); MS (APCI$^+$) m/z (%) = 494.2 (90) and 492.2 (100) $[M+H]^+$; Anal. Calcd for $C_{28}H_{46}BrNO$: C, 68.27, H, 9.41, N, 2.84. Found: C, 67.82, H, 9.52, N, 2.91.

2,6,10,15,19,23-Hexamethyl-tetracosa-1,6,10,14,18,22-hexaen-3-ol (11). To a stirred solution of 2,3-epoxysqualene **10** (5.18 g, 12 mmol) in toluene (60 mL) was added aluminium isopropoxide (7.40 g, 36 mmol). The resulting mixture was stirred under reflux for 16 h. After cooling to room temperature, 1 N HCl was added until the whole solid dissolved. The organic phase was separated and the aqueous phase extracted with diethyl ether (4 × 50 mL). The combined organic layers were washed with brine, dried over $MgSO_4$ and concentrated under reduced pressure. The resulting oily residue was purified by flash chromatographic purification over silica gel (petroleum ether/diethyl ether 4/1 v/v) to provide allylic alcohol **11** (3.26 g, 63%) as a colourless oil. IR (neat, cm^{-1}) ν = 3354, 2965, 2916, 2854, 1656, 1651, 1445, 1381, 1059, 1024, 993, 898, 837; ^{1}H NMR (300 MHz, $CDCl_3$) δ: 5.25–5.10 (m, 5H, HC═C), 4.96 (m, 1 H, H_2C═C), 4.86 (m, 1 H, H_2C═C), 4.05 (t, J = 6.5 Hz, 1 H, CHOH), 2.20–1.95 (m, 18 H, ═CCH_2CH_2), 1.75 (s, 3 H, H_2C═C(CH_3)), 1.70 (s, 3 H, ═C(CH_3)CH_2), 1.64 (s, 3H), 1.63 (s, 12 H, (CH_3)CH═); ^{13}C NMR (75 MHz, $CDCl_3$) δ: 147.4 (C), 134.9 (C), 134.8 (2 C), 134.5 (C), 131.0 (C), 124.7 (CH), 124.3 (2 CH), 124.2 (2 CH), 110.9 (CH_2), 75.5 (CH), 39.6 (3 CH_2), 35.6 (CH_2), 33.1 (CH_2), 28.2 (2 CH_2), 26.5 (3 CH_2), 25.6 (CH_3), 17.5 (2 CH_3), 15.9 (4 CH_3); MS (ESI$^+$) m/z (%) = 449.3 (100) $[M+Na]^+$. Anal. Calcd for $C_{30}H_{50}O.1/4\ H_2O$: C, 83.56; H, 11.80. Found: C, 83.95, H, 11.84.

4,8,12,17,21,25-Hexamethyl-hexacosa-4,8,12,16,20,24-hexaenoic acid ethyl ester (12). A stirred solution of alcohol **11** (2.74 g, 6.43 mmol) and propionic acid (0.05 g) in triethyl orthoacetate (40 mL) was heated at reflux temperature for 2 h. After cooling to room temperature Et_3N (0.07 g, 100 µL) was added and the mixture was concentrated under reduced pressure. The residue was stirred for 5 min with 0.1 N HCl solution (10 mL) and extracted with diethyl ether Et_2O (4 × 20 mL). The combined organic phases were washed with brine, dried over $MgSO_4$, filtered and concentrated under reduced pressure to provide the crude ester **12** (3.20 g, quantitative) as a pale yellow oil which was directly used in the next step without further purification. IR (neat, cm^{-1}) ν: 2917, 2852, 1738, 1448, 1382, 1297, 1252, 1155; ^{1}H NMR (300 MHz $CDCl_3$) δ: 5.20-5.02 (m, 6 H, HC═C), 4.09 (q, J = 7.2 Hz, 2 H, $CO_2CH_2CH_3$), 2.40-2.20 (m, 4 H, $CH_2CH_2CO_2Et$), 2.15-1.85 (m, 20 H, ═CCH_2CH_2), 1.66 (s, 3 H, (CH_3)$_2$C═), 1.59 (s, 18 H, ═C(CH_3)CH_2), 1.23 (t, J = 7.2 Hz, $CO_2CH_2CH_3$); ^{13}C NMR (75 MHz, $CDCl_3$) δ: 173.1 (C), 134.8 (2 C), 134.6 (C), 134.4 (C), 133.0 (C), 130.8 (C), 125.0 (CH), 124.3 (2 CH), 124.2 (3CH), 59.9 (CH_2), 39.6 (3 CH_2), 39.4 (CH_2), 34.5 (CH_2), 33.1 (CH_2), 28.1 (2 CH_2), 26.6 (CH_2), 26.5 (3 CH_2), 25.5 (CH_3), 17.5 (CH_3), 15.8 (4 CH_3), 14.1 (CH_3); MS (APCI$^+$) m/z (%) = 497.3 (100) $[M+H]^+$.

4,8,12,17,21,25-Hexamethyl-hexacosa-4,8,12,16,20,24-hexaen-1-ol (13a). To a stirred solution of the ester **12** (0.50 g, 1.0 mmol) in anhydrous THF (10 mL) cooled at −78 °C was added dropwise diisobutyl aluminium hydride (DIBAL-H; 1 M solution in cyclohexane, 2.4 mL, 2.4 mmol). After being stirred at the same temperature for 5 h, the reaction mixture was quenched by slow addition of methanol (1 mL). The reaction mixture was poured into aqueous Rochelle salt (tartaric acid potassium sodium salt 1 M, 20 mL, 20 mmol) and the resulting mixture was stirred for 24 h at 20 °C. The mixture was filtered and the filtrate concentrated under reduced pressure. The residue was taken in water then extracted with Et_2O (5 × 20 mL). The combined organic extracts were dried over $MgSO_4$ and concentrated *in vacuo*. The crude product was purified by flash chromatography on silica gel (cyclohexane/EtOAc, 4/1 v/v) to give the alcohol **13a** as a colourless oil (0.313 g, 69% yield): IR (neat, cm^{-1}) ν = 3600–3400, 2916, 1443, 1382, 1059, 837; ^{1}H NMR (300 MHz, $CDCl_3$) δ: 5.20–5.00 (m, 6 H, HC═C), 3.61 (t, J = 6.4 Hz, 2 H, CH_2OH), 2.15–1.90 (m, 24 H), 1.67 (s, 3 H, (CH_3)$_2$C═), 1.60 (s, 18 H, ═C(CH_3)CH_2). ^{13}C NMR (75 MHz, $CDCl_3$) δ: 135.0 (2 C), 134.8 (C), 134.7 (C), 134.5 (C), 131.1 (C), 124.7 (CH), 124.4 (2 CH), 124.3 (3 CH), 62.7 (CH_2), 39.7 (3 CH_2), 39.6 (CH_2), 35.9 (CH_2), 30.7 (CH_2), 28.2 (2 CH_2), 26.7 (CH_2), 26.6 (2 CH_2), 26.5 (CH_2), 25.6 (CH_3), 17.6 (CH_3), 16.0 (2 CH_3), 15.9 (2 CH_3), 15.8 (CH_3); MS (ESI$^+$) m/z (%) = 477.5 (100) $[M+Na]^+$. Anal. Calcd for $C_{32}H_{54}O.^1/_4\ H_2O$: C, 83.41; H, 11.96. Found: C, 83.68, H, 11.96.

2-(4,8,12,17,21,25-Hexamethyl-hexacosa-4,8,12,16,20,24-hexaenyl)-isoindole-1,3-dione (13c).

Method A: Gabriel Synthesis. To a solution of alcohol **13a** (0.41 g, 0.9 mmol), DMAP (0.024 g, 0.2 mmol) and anhydrous Et_3N (0.14 g, 1.35 mmol) in CH_2Cl_2 (3 mL) cooled at 0 °C was added dropwise mesyl chloride (0.124 g, 1.08 mmol) over 3 min. The mixture was stirred under nitrogen atmosphere at 0 °C for one more hour and overnight at room temperature. The organic phase was concentrated *in vacuo*. The residue was taken up in water (10 mL) and extracted with diethyl ether Et_2O (4 × 15 mL). The combined organic extracts were dried over $MgSO_4$, filtered and concentrated under reduced pressure to provide mesylate **13b** as a pale yellow oil (0.521 g). The crude product was used in the next step without further purification. IR (neat, cm^{-1}) ν = 2987, 2850, 1650, 1571, 1450, 1384, 1358, 1331, 1174; ^{1}H NMR (300 MHz, $CDCl_3$) δ: 5.20–5.05 (m, 6 H, HC═C), 4.19 (t, J = 6.5 Hz, 2 H, CH_2OMs), 3.00 (s, 3 H, SO_3CH_3), 2.15–1.95 (m, 20 H), 1.90–1.80 (m, 2H), 1.67 (s, 3 H, (CH_3)$_2$C═), 1.59 (s, 18 H, ═C(CH_3)CH_2).

To a stirred solution of the crude mesylate **13b** (0.5 g, 0.9 mmol) in anhydrous DMF (10 mL) was added portion-wise potassium phthalimide (0.33 g, 1.8 mmol) and the mixture was heated at 70 °C for 48 h. After cooling, the DMF was evaporated under vacuum. The oily residue was taken up in water (20 mL) and extracted with Et_2O (5 × 20 mL). The combined organic phases were washed with a solution of 0.1 N NaOH (3 × 15 mL) then brine (3 × 15 mL). The organic layer was dried over $MgSO_4$, filtered and concentrated *in vacuo*. The residue was purified by flash chromatography on silica gel (cyclohexane/EtOAc, 4/1 v/v), to afford **13c** as a yellow oil (0.45 g, 86% overall from **13a**).

Method B. To a solution of alcohol **13a** (0.95 g, 2.1 mmol), triphenylphosphine (0.66 g, 2.51 mmol) and phthalimide (0.37 g, 2.51 mmol), in THF (15 mL) was added dropwise at 0 °C a solution of diisopropylazodicarboxylate DIAD (0.534 g, 2.64 mmol) in THF (1 mL). After stirring for 15 h at 20 °C, ethanol (30 mL) was added and the mixture stirred for 1 h. The reaction mixture was then concentrated under reduced pressure. The residue was taken

up in 1 N aqueous ammonium chloride solution and extracted with EtOAc (4 × 25 mL). The combined organic phases were dried over $MgSO_4$, filtered and concentrated under reduced pressure. The residue was purified by flash chromatography on silica gel (cyclohexane/EtOAc, 4/1 v/v), to afford the phthalimide **13c** as a yellow oil (1.23 g, 86% yield). IR (neat, cm^{-1}) ν = 2978, 2927, 2852, 1774, 1713, 1451, 1436, 1395, 1366, 1333, 1122, 1040, 718; ^1H NMR (300 MHz, $CDCl_3$) δ: 7.85–7.80 (m, 2 H, H-4, H-7), 7.74–7.69 (m, 2 H, H-5, H-6) 5.20–5.05 (m, 6 H, *H*C═C), 3.65 (t, 2 H, J = 7.35 Hz, 2 H, NCH_2CH$_2$), 2.14–1.94 (m, 20 H), 1.88–1.72 (m, 2 H), 1.68 (s, 3 H, (CH_3)$_2$C═), 1.60 (s, 18 H, ═C(CH_3)CH$_2$); ^{13}C NMR (75 MHz, $CDCl_3$): 168.3 (2 C), 135.0 (2 C), 134.8 (C), 134.7 (C), 133.7 (2 CH), 133.5 (C), 132.1 (C), 131.1 (C), 125.0 (CH), 124.3 (2 CH), 124.2 (3 CH), 123.1 (2 CH), 39.7 (3 CH_2), 39.6 (CH_2), 37.8 (CH_2), 36.8 (CH_2), 28.2 (2 CH_2), 26.7 (CH_2), 26.6 (4 CH_2), 25.6 (CH_3), 17.6 (CH_3), 16.0 (2 CH_3), 15.9 (2 CH_3), 15.7 (CH_3); MS (ESI$^+$) m/z (%) = 606.4 (100) [M+Na]$^+$; Anal. Calcd for $C_{40}H_{57}NO_2$: C, 82.28, H, 9.84, N, 2.40 Found: C, 81.98, H, 9.44, N 2.58.

4,8,12,17,21,25-Hexamethyl-hexacosa-4,8,12,16,20,24-hexaenylamine (13d). To a solution of phthalimide **13c** (1.01 g, 1.74 mmol) in EtOH (40 mL) at 0 °C was added dropwise hydrazine monohydrate (0.5 g, 10 mmol). The reaction mixture was stirred at room temperature for 15 h. The solid formed was filtered (Whatman Filter Paper), and washed with a small amount of ethanol. The filtrate was concentrated under reduced pressure, and the resulting residue was taken up in water and extracted with EtOAc (5 × 20 mL). The combined organic phases were dried over $MgSO_4$, filtered and concentrated *in vacuo*. The residue was purified by flash chromatography on silica gel (cyclohexane/EtOAc/Et_3N, 20/10/0.05 v/v/v, EtOAc/Et_3N, 10/0.01v/v, EtOAc/MeOH/Et_3N 9/1/0.01 v/v/v) to provide amine **13d** as a pale yellow oil (0.68 g, 86% yield). IR (neat, cm^{-1}) ν = 3200–3000, 2926, 2849, 1443, 1381, 1036; ^1H NMR (300 MHz, CD_3OD) δ: 5.35–5.10 (m, 6 H, C*H*═C), 2.74 (t, J = 7.3 Hz, 2 H, NH$_2$CH_2CH$_2$), 2.35–2.00 (m, 24 H), 1.74 (s, 3 H, (CH_3)$_2$C═), 1.68 (s, 18 H, ═C(CH_3)CH$_2$); ^{13}C NMR (75 MHz, CD_3OD) δ: 136.0 (2 C), 135.8 (2 C), 135.3 (C), 132.0 (C), 129.3 (CH), 129.0 (CH), 125.0 (CH), 124.6 (3 CH), 41.8 (CH_2), 40.9 (4 CH_2), 38.0 (CH_2), 30.8 (CH_2), 29.3 (2 CH_2), 28.6 (CH_2), 27.9 (CH_2), 27.7 (2 CH_2), 26.1 (CH_3), 22.5 (2 CH_3), 18.0 (CH_3), 16.4 (3 CH_3); MS (ESI$^+$) m/z (%) = 454.4 (100) [M+Na]$^+$.

2-Bromo-*N*-(4,8,12,17,21,25-hexamethyl-hexacosa-4,8,12,16,20,24-hexaenyl)-acetamide (13e). To a vigorously stirred, ice-cooled solution of amine **13d** (0.07 g, 0.15 mmol) in CH_2Cl_2 (3 mL) and 1 N aqueous NaOH (3 mL, 3 mmol), bromoacetyl bromide (0.09 g, 0.45 mmol) was added dropwise and the reaction mixture was stirred at 0 °C for one more hour. The organic phase was concentrated under reduced pressure and the residue was taken up in H_2O (10 mL) and extracted with EtOAc (5 × 10 mL). The combined organic extracts were dried over $MgSO_4$, filtered and concentrated under reduced pressure. The oily residue was purified by flash chromatography on silica gel (cyclohexane/EtOAc, 2/1 v/v), to give bromoacetamide **13e** as a pale yellow oil (0.07 g, 80% yield). IR (neat, cm^{-1}) ν = 2924, 1720, 1450, 1376, 1246, 1178, 1107; ^1H NMR (300 MHz, $CDCl_3$) δ: 6.58 (broad s, 1 H, N*H*CO), 5.20–5.00 (m, 6 H, *H*C═C), 3.86 (s, 2 H, BrCH_2), 3.26 (m, 2 H, OCNHCH_2), 2.15–1.85 (m, 20 H), 1.67 (s, 3 H, (CH_3)$_2$C═), 1.59 (s, 18 H, ═C(CH_3)CH$_2$), 1.23 (m, 4H); ^{13}C NMR (75 MHz, $CDCl_3$) δ: 165.1 (C), 135.0 (2 C), 134.7 (C), 134.6 (C), 133.7 (C), 131.1 (C), 125.4 (CH), 124.3 (2 CH), 124.2 (3 CH), 39.8 (CH_2), 39.7 (4 CH_2), 39.6 (CH_2), 36.8 (CH_2), 29.3 (CH_2), 28.2 (2 CH_2), 27.1 (CH_2), 26.7 (CH_2), 26.6 (2 CH_2), 25.6 (CH_3), 17.6 (CH_3), 16.0 (2 CH_3), 15.9 (2 CH_3), 15.7 (CH_3); MS (ESI$^+$) m/z (%) = 576.2 (100) and 574.4 (95) [M+H]$^+$. Anal. Calcd for $C_{34}H_{56}BrNO$. $3^1/_2$ H_2O: C, 64.03; H, 9.96; N, 2.20. Found: C, 64.03, H, 9.14; N, 2.29.

[6-(2-Bromo-acetylamino)-hexyl]-carbamic acid *tert*-butyl ester (16). To a stirred, ice-cooled solution of *N*-(6-aminohexyl) carbamic acid *tert*-butyl ester (**15**) (0.20 g, 0.92 mmol) in CH_2Cl_2 (3 mL) and 1 N NaOH (3 mL, 3 mmol) was added dropwise bromoacetyl bromide (0.373 g, 1.85 mmol). After 45 min water (10 mL) was added and the mixture was extracted with CH_2Cl_2 (5 × 10 mL). The combined organic phases were dried over $MgSO_4$, filtered and concentrated under reduced pressure to leave the crude bromoacetamide **16** as a white waxy solid (0.31 g, quantitative). This compound was used in the next step without further purification. IR (neat, cm^{-1}) ν = 3299, 2930, 2857, 1675, 1534, 1465, 1390, 1365, 1283, 1252, 1213, 1168; ^1H NMR (300 MHz, $CDCl_3$) δ: 6.75 (broad s, 1H, N*H*CO), 4.65 (broad s, 1H, N*H*CO), 3.82 (s, 2H, BrCH_2), 3.25–3.00 (m, 4H, CONHCH_2), 1.60–1.35 (m, 11 H, CH_2, NHCOC(CH_3)$_3$), 1.30–1.00 (m, 4 H, CH_2); ^{13}C NMR (75 MHz, $CDCl_3$) δ: 165.4 (C), 156.0 (C), 79.0 (C), 40.2 (CH_2), 39.8 (CH_2), 39.7(CH_2), 29.8 (CH_2), 29.2 (CH_2), 29.0 (CH_2), 28.4 (3 CH_3), 26.0 (CH_2); MS (ESI$^+$) m/z (%) = 361 (100) and 359 (90), [M+Na]$^+$.

{4-[(6-*tert*-Butoxycarbonylamino-hexylcarbamoyl)-methyl]-7,10-bis-ethoxycarbonyl methyl-1,4,7,10 tetraaza-cyclododec-1-yl}-acetic acid ethyl ester (17a). A mixture of bromoacetamide **16** (0.173 g, 0.51 mmol), DO_3AEt (**8**) (0.20 g, 0.46 mmol), and potassium carbonate (0.075 g, 0.54 mmol) in anhydrous acetonitrile (3 mL) was heated at 70 °C for 24 h. After cooling, the reaction was filtered, the solid was thoroughly washed with CH_2Cl_2 and the filtrate was concentrated under reduced pressure. The residue was purified by flash chromatography on silica gel (CH_2Cl_2/EtOH/Et_3N, 9/1/0.05 v/v/v) to afford triester **17a** as a pale yellow viscous oil (0.214 g, 67% yield). IR (neat, cm^{-1}) ν = 2982, 2825, 1732, 1700, 1658, 1450, 1373, 1307, 1238, 1207, 1177, 1120, 1045; ^1H NMR (300 MHz, CD_3OD) δ: 4.30–4.15 (m, 6 H, OCH_2CH$_3$), 3.65–2.20 (m, 28 H), 1.65–1.40 (m, 13 H), 1.40–1.20 (m, 13H); ^{13}C NMR (75 MHz, CD_3OD) due to the amide resonance the splitting of some of the carbon lines was observed δ: 175.1 (C), 174.6 (2 C), 173.3 (C), 172.9 (C), 172.5 (C), 158.2 (C), 79.5 (C), 62.1 (CH_2), 62.0 (CH_2), 61.7 (CH_2), 61.6 (CH_2), 57.6 (CH_2), 56.8 (CH_2), 56.2 (CH_2), 56.1 (CH_2), 54.6 (CH_2), 53.0 (CH_2), 51.6 (CH_2), 50.1 (CH_2), 47.2 (CH_2), 41.2 (CH_2), 40.0 (CH_2), 30.8 (CH_2), 30.4 (CH_2), 28.9 (3 CH_3), 27.7 (CH_2), 27.5 (CH_2), 14.7 (2 CH_3), 14.6 (CH_3); MS (ESI$^+$) m/z (%) = 709.6 (100) [M+Na]$^+$, 431 (42) [DO_3AEt+H]$^+$. Anal. Calcd for $C_{33}H_{62}N_6O_9.KBr{\cdot}H_2O$: C, 48.11; H, 7.83; N, 10.20;. Found: C, 48.25; H, 7.87; N, 10.23.

{4-[(6-Amino-hexylcarbamoyl)-methyl]-7,10-bis-ethoxycarbonylmethyl-1,4,7,10 tetraaza-cyclododec-1-yl}-acetic acid ethyl ester (17b). To a solution of **17a** (0.17 g, 0.25 mmol) in CH_2Cl_2 (2 mL) and anisole (0.3 mL) was added dropwise trifluoroacetic acid (0.5 mL). The reaction was allowed to stir at room temperature for 4 h, then the reaction mixture was concentrated under reduced

pressure. The waxy residue was suspended in Et_2O (10 mL), filtered and washed with Et_2O (30 mL). The resulting waxy product was then taken up into saturated aqueous potassium hydrogen carbonate (10 mL) and the mixture was extracted with EtOAc (3 × 25 mL). The organic layer was dried over Na_2SO_4, filtered and concentrated under reduced pressure. The residue was purified by flash chromatography on silica gel (CH_2Cl_2/EtOH/Et_3N, 9/1/0.05 v/v/v) to afford amine **17b** as a yellow oil (0.12 g, 83% yield). IR (neat, cm^{-1}) ν = 2972, 2827, 1732, 1680, 1658, 1471, 1453, 1427, 1357, 1302, 1200, 1173, 1120, 1026, 833, 799, 775, 720; ^{1}H NMR (300 MHz, CD_3OD) δ: 4.20–4.05 (m, 6 H, OCH_2CH_3), 3.60–2.00 (m, 28 H), 1.80–1.40 (m, 8 H), 1.31 (t, J = 7.1 Hz, 9 H, OCH_2CH_3); ^{13}C NMR (75 MHz, CD_3OD) signals of cyclen moiety were hardly observed δ: 175.1 (C), 174.7 (2 C), 173.5 (C), 62.2 (3 CH_2), 57. 7 (CH_2), 56.2 (CH_2), 56.1 (2 CH_2), 40.9 (CH_2), 40.1 (CH_2), 30.3 (CH_2), 29.3 (CH_2), 27.5 (CH_2), 27.3 (CH_2), 14.6 (3 CH_3); MS (APCI$^+$) m/z (%) = 609 (15) [M+Na]$^+$, 587 (100) [M+H]$^+$.

4,8,12,17,21,25-Hexamethyl-hexacosa-4,8,12,16,20,24-hexaenoic acid (19). A solution of LiOH·H_2O (1.09 g, 25.9 mmol) in ethanol (30 mL) and THF (10 mL) was added to squaleneacetic acid ethyl ester (**12**) (3.24 g, 6.52 mmol) and heated at reflux temperature for 24 h. After cooling the reaction mixture was concentrated under reduced pressure and the residue was taken up in distilled water (10 mL) and acidified to pH 3 with 3 N HCl. The mixture was then extracted by Et_2O (5 × 20 mL). The combined organic extracts were dried over $MgSO_4$, filtered and concentrated under reduced pressure. The residue was purified by flash chromatography on silica gel (cyclohexane/EtOAc, 4/1 v/v) to provide squalenacetic acid **19**, as a pale yellow oil (2.53 g, 83% yield). IR (neat, cm^{-1}) ν = 2915, 1709, 1446, 1383, 1299, 1211; ^{1}H NMR (300 MHz, $CDCl_3$) δ: 5.20–5.05 (m, 6 H, HC═C), 2.45 (t, J = 6.5 Hz, 2 H, CH_2CO_2H), 2.30 (t, J = 7.1 Hz, 2 H, $CH_2CH_2CO_2H$), 2.15–1.95 (m, 20 H), 1.69 (s, 3 H, $(CH_3)_2C$═), 1.61 (s, 18 H, ═C(CH_3)CH_2). ^{13}C NMR (75 MHz, $CDCl_3$) δ: 179.8 (C), 135.0 (2 C), 134.8 (C), 134.6 (C), 132.8 (C), 131.2 (C), 125.3 (CH), 124.4 (2 CH), 124.3 (3 CH), 39.7 (3 CH_2), 39.5 (CH_2), 34.3 (CH_2), 33.0 (CH_2), 28.2 (2 CH_2), 26.9 (CH_2), 26.7 (CH_2), 26.6 (2 CH_2), 25.6 (CH_3), 17.6 (CH_3), 16.0 (2 CH_3), 15.9 (2 CH_3), 15.8 (CH_3); MS (ESI$^-$) m/z (%) = 467.4 (100) [M − H]$^-$. Anal. Calcd for $C_{32}H_{52}O_2$. $^1/_4$ H_2O: C, 81.21; H, 11.18. Found: C, 81.26; H, 11.23.

3,5-Bis-(4,8,13,17,21-pentamethyl-docosa-4,8,12,16,20-pentaenoylamino)-benzoic acid methyl ester (22a). To an ice-cooled stirred solution of the trisnor-squalenic acid **5** (0.60 g, 1.51 mmol) and DMAP (0.024 g, 0.2 mmol) in anhydrous THF (6 mL) was added dropwise Et_3N (0.18 g, 1.8 mmol) and ethyl chloroformate (0.18 g, 1.65 mmol). The mixture was stirred at 0 °C for 30 min then a solution of methyl 3,5-diaminobenzoate **21** (0.10 g, 0.6 mmol) in (THF/CH_2Cl_2, 1/1 v/v, 3 mL) was added. The reaction mixture was stirred for 24 h at room temperature then concentrated under reduced pressure. The oily residue was taken up in saturated aqueous potassium hydrogen carbonate (20 mL) and the mixture was extracted with EtOAc (4 × 30 mL). The combined extracts were washed with water, dried over $MgSO_4$, filtered and concentrated under reduced pressure. The crude product was purified by flash chromatography on silica gel (cyclohexane/EtOAc, 1/2 v/v) to provide pure methyl 3,5-bis-squalenoylamino-benzoate **22a** as a viscous colourless oil (0.475 g, 85% yield). IR (neat, cm^{-1}) ν = 2915, 1722, 1669, 1606, 1556, 1449, 1380, 1229; ^{1}H NMR (300 MHz, CD_3OD) δ: 7.46 (t, J = 1.5 Hz, 1 H, H-4), 7.29 (t, J = 2.0 Hz, 1 H), 7.11 (t, J = 1.7 Hz, 1 H), 5.24 (t, J = 6.6 Hz, 2 H, HC═C), 5.20–5.05 (m, 8 H, HC═C), 3.86 (s, 3H, CO_2CH_3), 2.50–2.30 (m, 8 H, CH_2CH_2NHCO), 2.20–1.90 (m, 32 H), 1.68 (s, 6 H, $(CH_3)_2C$═), 1.50 (m, 30 H, ═C(CH_3)CH_2); ^{13}C NMR (75 MHz, $CDCl_3$) δ: 173.5 (C), 171.4 (2 C), 138.7 (2 C), 135.0 (4 C), 134.8 (C), 134.6 (2 C), 133.2 (2 C), 131.2 (2 C), 125.8 (2 CH), 125.1 (2 CH), 124.2 (6 CH), 116.2 (2 CH), 115.1 (CH), 52.2 (CH3), 39.7 (4 CH_2), 39.5 (2 CH_2), 36.2 (CH_2), 35.0 (CH_2), 34.6 (2 CH_2), 33.3 (2 CH_2), 28.2 (4 CH_2), 26.6 (4 CH_2), 25.6 (2 CH_3), 17.6 (2 CH_3), 16.0 (6 CH_3), 14.2 (2 CH_3); MS (ESI$^-$) m/z (%) = 930.0 (100) [M − H]$^-$. Anal. Calcd for $C_{61}H_{92}N_2O_4$. $1^1/_4$ H_2O: C, 77.58; H, 10.14; N, 2.97. Found: C, 77.58; H, 9.91; N, 2.88.

3,5-Bis-(4,8,13,17,21-pentamethyl-docosa-4,8,12,16,20-pentaenoylamino)-benzoic acid (22b). A solution of methyl 3,5-bis-squalenoylamino-benzoate **22a** (0.475 g, 0.51 mmol) in (THF/ethanol, 2/1 v/v, 12 mL) was treated with LiOH·H_2O (0.09 g, 2.14 mmol). The mixture was heated at reflux temperature for 3 h. After cooling, the reaction mixture was concentrated under reduced pressure. The residue was taken up into distilled water (10 mL), 3 N HCl was added to modify the pH (pH = 3) and the mixture was extracted with EtOAc (5 × 20 mL). The combined organic phases were dried over $MgSO_4$, filtered and concentrated under reduced pressure. The residue was purified by flash chromatography on silica gel (cyclohexane/EtOAc, 2/1 v/v then 1/4) to provide the acid **22b** as a thick colorless oil (0.34 g, 72% yield). IR (neat, cm^{-1}) ν = 3330–3000, 2967, 2912, 1714, 1651, 1612, 1539, 1452, 1418, 1380, 1326, 1270, 1204; ^{1}H NMR (300 MHz, CD_3OD) δ: 8.20 (t, J = 1.8 Hz, 1 H, H-4), 7.98 (t, J = 1.8 Hz, 2 H, H-2, H-6), 5.24 (t, J = 6.6 Hz, 2 H, HC═C), 5.17–5.08 (m, 8 H, HC═C), 2.56–2.35 (m, 8 H, OCNHCH_2CH_2), 2.20–1.92 (m, 32 H), 1.70 (s, 6H, $(CH_3)_2C$═), 1.61 (s, 30 H, (═C(CH_3)CH_2); ^{13}C NMR (75 MHz, CD_3OD) δ: 174.3 (2 C), 169.4 (C), 140.6 (2 C), 136.0 (2 C), 135.9 (2 C), 135.8 (2 C), 134.6 (4 C), 133.0 (2 C), 132.0 (C), 126.5 (2 CH), 125.6 (6 CH), 125.5 (2 CH), 117.9 (2 *C*H), 116.9 (CH), 40.9 (4 CH_2), 40.7 (2 CH_2), 37.1 (2 CH_2), 36.7 (2 CH_2), 29.3 (4 CH_2), 27.9 (2 CH_2), 27.7 (2 CH_2), 27.6 (2 CH_2), 26.0 (2 CH_3), 17.9 (2 CH_3), 16.3 (4 CH_3), 16.2 (2 CH_3) 16.1 (2 CH_3); MS (ESI$^-$) m/z (%) = 916.0 (100) [M − H]$^-$.

Triethyl 2,2′,2″-[10-(2-oxo-2-{[3,7,12,16,20-pentamethylhenicosa-3,7,11,15,19-pentaen-1-yl]amino}ethyl)-1,4,7,10-tetraazacyclododecane-1,4,7-triyl] triacetate (9a). A mixture of DO_3AEt (**8**) (0.50 g, 1.16 mmol), bromoacetamide **7c** (0.63 g, 1.27 mmol) and potassium carbonate (0.20 g, 1.45 mmol) in anhydrous acetonitrile (3 mL) was heated to 60 °C for 48 h. After cooling, the reaction was filtered, the solid was washed with CH_2Cl_2, and the filtrate was concentrated under reduced pressure. The residue was purified by flash chromatography on silica gel (CH_2Cl_2/EtOH/Et_3N, 9/1/0.05 v/v/v) to give the expected triester **9a** (0.80 g, 82%) as a yellow viscous oil. IR (neat, cm^{-1}) ν = 3500–3000 (broad), 2913, 2844, 1733, 1661, 1554, 1451, 1380, 1306, 1106, 1028; ^{1}H NMR (300 MHz, C_6D_6) δ: 10.00 (t, J = 5.2 Hz, 1 H, NHCO), 5.50–5.20 (m, 5 H, HC═C), 4.09–1.90 (m, 50 H), 1.69 (s, 3 H), 1.68 (s, 3 H), 1.65 (s, 3 H), 1.64 (s, 3 H), 1.62 (s, 3 H), 1.58 (s, 3 H), 1.00 (t, J = 7.1 Hz, 6 H), 0.93 (t, J = 7.1 Hz, 3 H); ^{13}C NMR (75 MHz, C_6D_6) δ: 174.8 (C), 173.2 (2 C), 172.7 (C), 135.5 (C), 135.1 (C), 134.9 (C), 133.4 (C), 131.0 (C), 125.8

(CH), 124.9 (2 CH), 124.8 (CH), 124.4 (CH), 60.9 (3 CH_2), 57.1 (CH_2), 55.6 (3 CH_2), 53.0–49.0 (broad m, 8 CH_2), 40.3 (CH_2), 40.2 (2 CH_2), 39.8 (CH_2), 38.6 (CH_2), 28.7 (2 CH_2), 27.5 (CH_2), 27.2 (CH_2), 27.1 (CH_2), 25.8 (CH_3), 17.7 (CH_3), 16.3 (2 CH_3), 16.2 (CH_3), 16.1 (CH_3), 14.6 (2 CH_3), 14.3 (CH_3); MS (ESI^+) *m/z* (%) = 879.2 (5) $[M+K]^+$; 865.3 (100) $[M+Na]^+$; Anal. Calcd for $C_{48}H_{83}N_5O_7$.KBr. C 59.98, H 8.70, N 7.29 Found: C, 60.01, H, 8.82, N, 7.38.

{4,7-Bis-ethoxycarbonylmethyl-10-[(4,8,12,17,21,25-hexamethyl-hexacosa-4,8,12,16,20,24-hexaenylcarbamoyl)-methyl]-1,4,7,10-tetraaza-cyclododec-1-yl}-acetic acid ethyl ester (14a). A mixture of DO_3AEt (**8**) (0.14 g, 0.33 mmol), bromoacetamide **13e** (0.21 g, 0.36 mmol) and potassium carbonate (0.06 g, 0.41 mmol) in anhydrous acetonitrile (2 mL) was heated at 60 °C for 48 h. After cooling, the reaction was filtered, the solid was washed with CH_2Cl_2, and the filtrate was concentrated under reduced pressure. The residue was purified by flash chromatography on silica gel (CH_2Cl_2/EtOH/Et_3N, 9/1/0.05 v/v/v) to give the triester **14a** (0.236 g, 78%) as a yellow viscous oil. IR (neat, cm^{-1}) ν = 2921, 2851, 1662, 1558, 1306, 1204, 974; ^1H NMR (300 MHz, CD_3OD) δ: 5.25–5.05 (m, 6 H, *H*C═C), 4.30–4.18 (m, 6 H, OC*H*$_2$CH$_3$), 3.60–2.20 (m, 26 H), 2.20–1.85 (m, 24 H), 1.66 (s, 3H, (C*H*$_3$)$_2$C═), 1.55 (s, 18 H, ═C(C*H*$_3$)CH$_2$), 1.35–1.25 (m, 9H, OCH$_2$C*H*$_3$); ^{13}C NMR (75 MHz, CD_3OD) signals of cyclen moiety were hardly observed δ: 175.3 (C), 174.8 (2 C), 173.5 (C), 136.0 (2 C), 135.8 (2 C), 135.4 (C), 132.1 (C), 125.9 (CH), 125.6 (2 CH), 125.5 (CH), 125.4 (2 CH), 62.3 (CH_2), 62.2 (2 CH_2), 57.7 (CH_2), 56.3 (CH_2), 56.1 (CH_2), 40.9 (2 CH_2), 40.1 (CH_2), 38.1 (CH_2), 29.1 (CH_2), 29.0 (CH_2), 27.9 (CH_2), 27.8 (CH_2), 27.6 (CH_2), 26.4 (CH_2), 26.0 (CH_3), 20.1 (CH_3), 17.9 (CH_3), 16.3 (2CH_3), 16.2 (CH_3), 14.7 (3CH_3), 14.6 (CH_3); MS (ESI^+) *m/z* (%) = 947 (100) $[M+Na]^+$.

(4,7-Bis-ethoxycarbonylmethyl-10-{[6-(4,8,13,17,21-pentamethyl-docosa-4,8,12,16,20-pentaenoylamino)-hexylcarbamoyl]-methyl}-1,4,7,10-tetraaza-cyclododec-1-yl)-acetic acid ethyl ester (18a). A stirred solution of trisnor-squalenic acid derivative **5** (0.123 g, 0.3 mmol) and Et_3N (0.04 g, 0.38 mmol) in anhydrous CH_2Cl_2 (10 mL $mmol^{-1}$) was cooled to 0 °C and a solution of ethyl chloroformate (0.04 g, 0.34 mmol) was added dropwise. The mixture was stirred at 0 °C for 25 min, and a solution of cyclen **17b** (0. 12 g, 0.2 mmol) and DMAP (0.01 g, 0.08 mmol) in anhydrous CH_2Cl_2 (10 mL $mmol^{-1}$) was added dropwise at the same temperature. The reaction mixture was stirred for 1 h at 0 °C then 24 h at room temperature and then concentrated under reduced pressure. Aqueous potassium hydrogen carbonate was added to the residue and the mixture was extracted with EtOAc. The combined organic phase was washed with water, dried over Na_2SO_4, and concentrated under reduced pressure. The residue was purified by flash chromatography on silica gel (CH_2Cl_2/EtOH/NH_4OH, 9/1/0.05 v/v/v) to give the expected triesters **18a**, (0.14 g, 72%) as a yellow viscous oil. IR (neat, cm^{-1}) ν = 3500–3000 (broad), 3253, 2932, 2856, 1733, 1655, 1580, 1537, 1438, 1382, 1307, 1199, 1107; ^1H NMR (300 MHz, CD_3OD) δ: 7.93 (t, *J* = 8.7 Hz, 1 H, N*H*CO), 5.25–5.05 (m, 5 H, *H*C═C), 4.35–4.10 (m, 6 H, OC*H*$_2$CH$_3$), 3.70–2.15 (m, 32 H), 2.12–1.90 (m, 18 H), 1.69 (s, 3 H, (C*H*$_3$)$_2$C═), 1.65 (s, 3 H, (C*H*$_3$)$_2$C═), 1.62 (s, 12 H, ═C(C*H*$_3$)CH$_2$), 1.60–1.45 (m, 4 H, OCNHCH$_2$C*H*$_2$), 1.44–1.35 (m, 4 H, OCNHCH$_2$CH$_2$C*H*$_2$), 1.30 (t, *J* = 7.6 Hz, 9H, CO$_2$CH$_2$C*H*$_3$); ^{13}C NMR (75 MHz, CD_3OD) signals of cyclen moiety were hardly observed δ: 175.6 (C), 175.3 (C), 174.8 (2 C), 173.4 (C), 136.0 (2 C), 135.8 (C), 134.9 (C), 132.1 (C), 126.2 (CH), 125.6 (2 CH), 125.5 (2 CH), 62.3 (CH_2), 62.2 (2 CH_2), 57.7 (CH_2), 56.3 (CH_2), 56.1 (CH_2), 40.9 (CH_2), 40.8 (CH_2), 40.3 (CH_2), 40.2 (CH_2), 36.9 (CH_2), 36.2 (CH_2), 30.5 (CH_2), 30.4 (CH_2), 29.3 (2 CH_2), 27.9 (CH_2), 27.8 (CH_2), 27.7 (2 CH_2), 27.6 (CH_2), 26.0 (CH_3), 17.9 (CH_3), 16.3 (2 CH_3), 16.2 (CH_3), 16.1 (CH_3), 14.7 (2 CH_3), 14.6 (CH_3); MS ($APCI^+$) *m/z* (%) = 970 (100) $[M+H]^+$.

(4,7-Bis-ethoxycarbonylmethyl-10-{[6-(4,8,12,17,21,25-hexamethyl-hexacosa-4,8,12,16,20,24-hexaenoylamino)-hexylcarbamoyl]-methyl}-1,4,7,10 tetraaza-cyclododec-1-yl)-acetic acid ethyl ester (20a). Condensation of **19** (0.24 g, 0.51 mmol) and **17b** (0.2 g, 0.34 mmol) according to the procedure used for **18a** gave triester **20a** (0.24 g, 68%) as a yellow viscous oil. IR (neat, cm^{-1}) ν = 3500–3300, 3000–2800, 1734, 1692, 1666, 1554, 1452, 1381, 1306, 1263, 1199, 1176, 1121, 1106, 1051; ^1H NMR (300 MHz, CD_3OD) δ: 5.25–5.05 (m, 6 H, *H*C═C), 4.35–4.10 (m, 6 H, OC*H*$_2$CH$_3$), 3.80–2.20 (m, 32 H), 2.15–1.90 (m, 20 H) 1.68 (s, 3 H, ═C(C*H*$_3$)$_2$), 1.55 (s, 18 H, ═C(C*H*$_3$)CH$_2$), 1.50–1.40 (m, 4 H, OCNHCH$_2$C*H*$_2$), 1.40–1.30 (m, 4 H, OCNHCH$_2$CH$_2$C*H*$_2$), 1.40–1.10 (m, 9 H, CO$_2$CH$_2$C*H*$_3$); ^{13}C NMR (75 MHz, CD_3OD) signals of cyclen moiety were hardly observed δ: 175.6 (C), 175.3 (C), 174.8 (2 C), 173.4 (C), 136.0 (2 C), 135.8 (2 C), 134.8 (C), 132.0 (C), 126.2 (CH), 125.8 (CH), 125.6 (3 CH), 125.5 (CH), 62.25 (CH_2), 62.2 (2 CH_2), 57.7 (CH_2), 56.3 (CH_2), 56.1 (CH_2), 47.8 (2 CH_2), 40.9 (2 CH_2), 40.8 (CH_2), 40.3 (CH_2), 40.2 (CH_2), 36.9 (CH_2), 36.4 (CH_2), 36.2 (CH_2), 35.2 (CH_2), 30.5 (CH_2), 30.4 (CH_2), 29.3 (2 CH_2) 27.9 (2 CH_2), 27.8 (CH_2), 27.7 (2 CH_2), 27.6 (CH_2), 26.6 (CH_3), 17.9 (CH_3), 16.3 (3 CH_3), 16.2 (CH_3), 16.1 (CH_3), 14.7 (2 CH_3), 14.6 (CH_3); MS (ESI^+) *m/z* (%) = 1060.5 (100) $[M+Na]^+$.

[4-({6-[3,5-Bis-(4,8,13,17,21-pentamethyl-docosa-4,8,12,16,20-pentaenoylamino)-benzoylamino]-hexylcarbamoyl}-methyl)-7,10-bis-ethoxycarbonylmethyl-1,4,7,10-tetraaza-cyclododec-1-yl]-acetic acid ethyl ester (23a). To a stirred solution of the acid **22b** (0.205 g, 0.22 mmol) in anhydrous CH_2Cl_2 (15 mL), were sequentially added the amine **17b** (0.18 g, 0.31 mmol), EDCI·HCl (0.10 g, 0.52 mmol) and DMAP (0.032 g, 0.26 mmol). The reaction mixture was stirred at room temperature for 72 h and was then concentrated under reduced pressure. The residue was taken up into 10 mL of MilliQ water and extracted with EtOAc (5 × 20 mL). The combined organic layers were dried over Na_2SO_4, filtered and concentrated *in vacuo*. The oily residue was purified by flash chromatography on silica gel (CH_2Cl_2/Et_3N 1/0.01 v/v, CH_2Cl_2/EtOH/Et_3N 9/1/0.1 v/v/v) to give **23a** as pale yellow viscous oil (0.237 g, 73% yields). IR (neat, cm^{-1}) ν = 3400–3200, 2935, 2855, 1734, 1689, 1662, 1644, 1600, 1562, 1451, 1380, 1309, 1263, 1213, 1200, 1176, 1122, 1106; ^1H NMR (300 MHz, CD_3OD) δ: 7.96 (s, 1 H, H-4), 7.77 (s, 2 H, H-2, H-6), 5.21 (t, *J* = 6.5 Hz, 2 H, *H*C═C), 5.16–5.00 (m, 8 H, *H*C═C), 4.30–4.15 (m, 6 H, CO$_2$C*H*$_2$CH$_3$), 3.45–2.60 (m, 28 H), 2.58–2.46 (m, 8 H), 2.20–1.98 (m, 32 H), 1.69 (s, 6 H, (C*H*$_3$)$_2$C═), 1.62 (s, 30 H, ═C(C*H*$_3$)CH$_2$), 1.60–1.40 (m, 4 H, OCNHCH$_2$C*H*$_2$), 1.40–1.30 (m, 4 H, OCNHCH$_2$CH$_2$C*H*$_2$), 1.40–1.20 (m, 9 H, CO$_2$CH$_2$C*H*$_3$); ^{13}C NMR (75 MHz, CD_3OD) signals of cyclen moiety were hardly observed δ: 175.3 (C), 174.7 (2 C), 174.2 (2 C), 173.4 (C), 169.7 (C), 140.6 (2 C), 137.2 (C), 136.0 (2 C), 135.9 (2 C), 135.8 (2 C), 134.7 (2 C), 132.0 (2 C), 126.4 (2 CH), 125.6 (4 CH), 125.5 (4 CH), 116.9

(2 CH), 115.5 (CH), 62.2 (3 CH_2), 58.3 (CH_2), 57.7 (CH_2), 57.1 (CH_2), 56.3 (CH_2), 56.1 (CH_2), 53.8 (broad, CH_2), 47.9 (CH_2), 40.9 (CH_2), 40.8 (CH_2), 40.2 (CH_2), 37.1 (CH_2), 36.6 (CH_2), 30.5 (CH_2), 30.4 (CH_2), 29.3 (CH_2), 27.9 (CH_2), 27.8 (CH_2), 27.7 (CH_2), 26.0 (2 CH_3), 17.9 (2 CH_3), 16.4 (4 CH_3), 16.3 (2 CH_3), 16.2 (2 CH_3), 14.7 (2 CH_3), 14.6 (CH_3); MS (ESI^+) m/z (%) = 1509.1 (70) $[M+Na]^+$, 681.8 (100).

General procedure for the hydrolysis of the triester cyclens

To a carefully degassed solution of the given triester (1 equiv.) in a methanol/THF mixture (1/2 v/v, 30 mL $mmol^{-1}$) was added dropwise a solution of lithium hydroxide $LiOH{\cdot}H_2O$ (4 equiv.) in Milli-Q water (2 mL $mmol^{-1}$). After stirring for 15 h at room temperature, the mixture was concentrated under reduced pressure. The residue was suspended in Milli-Q water (15 mL), and the pH modified with 1 N HCl (pH = 5). The obtained solution was dialyzed against Milli-Q water with a cellulose ester dialysis membrane (MWCO = 500 Dalton) for 24 h, and was then freeze dried to give the corresponding triacid.

2,2′,2″-[10-(2-Oxo-2-{[3,7,12,16,20-pentamethylhenicosa-3,7,11,15,19-pentaen-1-yl]amino}ethyl)-1,4,7,10-tetraazacyclododecane-1,4,7-triyl]triacetic acid (9b). Hydrolysis of **9a** (0.564 g, 0.665 mmol) according to the general procedure gave **9b** as a white amorphous solid (0.327 g, 64% yields). IR (neat, cm^{-1}) ν = 3600–2900 broad, 1680–1580, 1400, 1220, 1153, 1087; ^{1}H NMR (400 MHz, CD_3OD) δ: 5.30–5.00 (m, 5 H, $HC{=}C$), 4.00–2.50 (m, 28 H), 2.18 (t, J = 4.0 Hz, 2H), 2.12–1.93 (m, 14 H), 1.66 (s, 3H), 1.64 (s, 3H), 1.59 (s, 12H); ^{13}C NMR (100 MHz, CD_3OD) δ: 177.2 (C), 177.0 (2 C) 171.6 (C), 136.0 (C), 135.9 (C), 135.8 (C), 133.5 (C), 132.0 (C), 127.4 (CH), 125.6 (CH), 125.5 (3 CH), 58.5–56.5 (broad m, 4 CH_2), 53.0–49.0 (broad m, 8 CH_2), 40.8 (3 CH_2), 40.4 (CH_2), 39.2 (CH_2), 29.2 (2 CH_2), 27.9 (CH_2), 27.8 (CH_2), 27.5 (CH_2), 25.9 (CH_3), 17.8 (CH_3), 16.3 (CH_3), 16.2 (2 CH_3), 16.1 (CH_3); MS (ESI^-) m/z (%) = 794.8 (74) $[M+K-2H]^-$, 779.8 (36) $[M+Na-2H]^-$, 756 (100) $[M-H]^-$.

{**4,7-Bis-carboxymethyl-10-[(4,8,12,17,21,25-hexamethyl-hexacosa-4,8,12,16,20,24-hexaenylcarbamoyl)-methyl]-1,4,7,10-tetraaza-cyclododec-1-yl}-acetic acid (14b).** Hydrolysis of **14a** (0.23 g, 0.25 mmol) according to the general procedure gave **14b** as a white amorphous solid (0.157 g, 76%). IR (neat, cm^{-1}) ν = 3600–3100 (broad), 2915, 1635, 1596, 1384, 1162, 1090; ^{1}H NMR (300 MHz, CD_3OD) δ: 5.20–5.10 (m, 6 H, $HC{=}C$), 3.20–2.30 (m, 26 H), 2.20–1.90 (m, 22 H), 1.66 (s, 3H, $(CH_3)_2C{=}$), 1.55 (m, 20 H, $CONHCH_2CH_2$, $HC{=}C(CH_3)$); ^{13}C NMR (75 MHz, CD_3OD) signals of cyclen moiety were hardly observed δ: 178.2 (3 C), 173.1 (C), 136.0 (2 C), 135.9 (C), 135.8 (2 C), 132.0 (C), 126.1 (CH), 125.6 (2 CH), 125.5 (3 CH), 59.4 (m, broad, CH_2), 53.0–51.0 (m, broad, CH_2), 40.9 (3 CH_2), 40.5 (CH_2), 38.3 (CH_2), 29.3 (2 CH_2), 28.8 (CH_2), 27.9 (2 CH_2), 27.7 (CH_2), 27.6 (CH_2), 26.0 (CH_3), 20.2 (CH_3), 17.9 (CH_3), 16.3 (3 CH_3), 16.2 (CH_3); MS (ESI^+) m/z (%) = 862.6 (100) $[M+Na]^+$.

(4,7-Bis-carboxymethyl-10-{[6-(4,8,13,17,21-pentamethyl-docosa-4,8,12,16,20-pentaenoylamino)-hexylcarbamoyl]-methyl}-1,4,7,10-tetraaza-cyclododec-1-yl)-acetic acid (18b). Hydrolysis of **18a** (0.067 g, 0.076 mmol) according to the general procedure gave **18b** as a white amorphous solid (0.047 g, 76%). IR (neat, cm^{-1}) ν = 3500–3100 (broad), 2923, 1637, 1510, 1440, 1384, 1205, 1148, 1087; ^{1}H NMR (300 MHz, CD_3OD) δ: 5.25–5.00 (m, 5 H, $HC{=}C$), 3.80–2.20 (m, 32 H), 2.16–1.92 (m, 16 H), 1.67 (s, 3 H), 1.64 (s, 3 H), 1.60 (s, 12 H), 1.60–1.50 (m, 4 H, $OCNHCH_2CH_2$), 1.40–1.30 (m, 4 H, $OCNHCH_2CH_2CH_2$); ^{13}C NMR (75 MHz, CD_3OD) signals of cyclen moiety were hardly observed δ: 175.6 (3 C), 135.9 (C), 135.8 (C), 134.9 (2 C), 132.0 (C), 126.1 (CH), 125.6 (CH), 125.5 (CH), 125.4 (2 CH), 59.0 (m, broad, CH_2), 53.0–50.5 (m, broad, CH_2), 40.8 (3 CH_2), 40.5 (CH_2), 40.3 (CH_2), 36.9 (CH_2), 36.2 (CH_2), 30.3 (CH_2), 30.1 (CH_2), 29.2 (2 CH_2), 27.8 (2 CH_2), 27.7 (CH_2), 27.6 (CH_2), 27.5 (CH_2), 26.0 (CH_3), 17.9 (CH_3), 16.4 (CH_3), 16.36 (CH_3), 16.3 (CH_3), 16.2 (CH_3); (ESI^+) m/z (%) = 891.9 (45) $[M+Li]^+$, 885.9 (100) $[M+H]^+$.

(4,7-Bis-carboxymethyl-10-{[6-(4,8,12,17,21,25-hexamethyl-hexacosa-4,8,12,16,20,24-hexaenoylamino)-hexylcarbamoyl]-methyl}-1,4,7,10-tetraaza-cyclododec-1-yl)-acetic acid (20b). Hydrolysis of **20a** (0.195 g, 0.19 mmol) according to the general procedure gave **20b** as a white amorphous solid (0.127 g, 71% yields). IR (neat, cm^{-1}) ν = 3600–3200 (broad), 2920, 1644, 1440, 1382, 1161, 1090. ^{1}H NMR (300 MHz, CD_3OD) δ: 5.25–5.05 (m, 6 H, $HC{=}C$), 3.70–2.15 (m, 32 H), 2.15–1.90 (m, 20 H) 1.70–1.40 (m, 25 H), 1.40–1.15 (m, 4 H); ^{13}C NMR (75 MHz, CD_3OD) signals of cyclen moiety were hardly observed δ: 176.2 (3 C), 172.1 (2C), 136.0 (2C), 135.9 (C), 134.9 (2 C), 132.4 (C), 126.2 (CH), 126.1 (CH), 125.6 (2 CH), 125.5 (2 CH), 58.1 (m, broad, 3 CH_2), 57.0 (2 CH_2), 53.0–52.3 (m, broad, CH_2), 40.9 (3 CH_2), 40.4 (2 CH_2), 36.9 (CH_2), 36.2 (CH_2), 35.9 (CH_2), 30.8 (CH_2), 30.3 (2 CH_2), 29.2 (2 CH_2), 27.6 (5 CH_2), 26.0 (CH_3), 17.8 (CH_3), 16.2 (5 CH_3); MS (ESI^+) m/z (%) = 961 (50) $[M+Li]^+$, 954 (100) $[M+H]^+$.

[4-({6-[3,5-Bis-(4,8,13,17,21-pentamethyl-docosa-4,8,12,16,20-pentaenoylamino)-benzoylamino]-hexylcarbamoyl}-methyl)-7,10-bis-carboxymethyl-1,4,7,10-tetraaza-cyclododec-1-yl]-acetic acid (23b). Hydrolysis of **23a** (0.089 g, 0.06 mmol) according to the general procedure using 6 equiv. of $LiOH{\cdot}H_2O$ gave **23b** as a white amorphous solid (0.07 g of the crude product). IR (neat, cm^{-1}) ν = 3600–3200 (broad), 2919, 1643, 1598, 1443, 1371, 1214, 1091; ^{1}H NMR (300 MHz, CD_3OD) δ: 7.94 (s, 1 H, H-4), 7.75 (s, 2H, H-2, H-6), 5.24 (t, J = 6.3 Hz, 2 H, $HC{=}C$), 5.17–5.05 (m, 8 H, $HC{=}C$), 3.50–2.20 (m, 36 H), 2.20–1.92 (m, 32 H), 1.69 (s, 3H, $(CH_3)_2C{=}$), 1.60 (m, 36 H, $=C(CH_3)CH_2$, $OCNHCH_2CH_2$), 1.50–1.40 (m, 4 H, $OCNHCH_2CH_2CH_2$); ^{13}C NMR (75 MHz, CD_3OD) signals of cyclen moiety were hardly observed δ: 174.3 (2C), 174.1 (2 C), 173.9 (C), 173.1 (C), 169.8 (C), 140.6 (2 C), 137.2 (C), 135.9 (4 C), 135.8 (2 C), 134.7 (2 C), 132.0 (2 C), 126.5 (2 CH), 125.6 (4 CH), 125.5 (4 CH),117.9 (CH), 115.5 (2 CH), 56.1 (CH_2), 53.0–51.5 (m, CH_2), 40.9 (4 CH_2), 40.7 (2 CH_2), 37.1 (2 CH_2), 36.7 (2 CH_2), 30.8 (CH_2), 30.3 (CH_2), 30.2 (CH_2), 29.3 (4 CH_2), 27.9 (2 CH_2), 27.8 (2 CH_2), 27.6 (2 CH_2), 26.1 (2 CH_3), 17.9 (2 CH_3), 16.3 (4 CH_3), 16.2 (4 CH_3); MS (ESI^+) m/z (%) = 1425 (20) $[M+Na]^+$, 1403 (100) $[M+H]^+$.

General procedure for the synthesis of gadolinium complexes

A solution of gadolinium chloride hexahydrate $GdCl_3{\cdot}6H_2O$ (1.1 equiv.) in Milli-Q water (2 mL $mmol^{-1}$) was added dropwise to a solution of cyclen triacid (1.0 equiv.) in Milli-Q water (15 mL $mmol^{-1}$). The pH of the solution was continuously adjusted between 6 and 7 by addition of 1 N NaOH (the pH was reduced to 3.8 when $GdCl_3$ was added). Once all $GdCl_3$ had been added,

the pH was maintained at 6.5 and the reaction mixture was stirred for 60 h at room temperature for **2** and **3** and 24 h at 50 °C for **4a–c**. The solution was then dialyzed against Milli-Q with a cellulose ester dialysis membrane (MWCO = 500 Dalton) for 24 h, then freeze dried. The white powder obtained was further purified by reversed-phase chromatography on a C-18 grafted silica gel eluting with methanol under pressure. The collected fractions were analyzed using a RP18 (F_{254}) silica gel TLC plate visualised with I_2, eluting with methanol. The suitable fractions were combined and concentrated under reduced pressure. If there is a trace of Gd^{3+} ions, the solution of Gd^{3+} complex in water was stirred with chelex100 (sodium form) at PH between 6 and 7, the pH of chelex was modified with amberlite IR 120, (H form). The absence of free Gd^{3+} ions was tested by using a xylenol orange indicator.[25] The fractions containing the pure complex were collected and concentrated under vacuum. The solid residue was taken-up into Milli-Q water (100 mL $mmol^{-1}$), and the solution was then freeze-dried to deliver the gadolinium complex as an amorphous white solid. The purity and the Gd^{3+} content of the complex were assessed by Evans' method [16,53] and inductive coupled plasma atomic emission (ICP-AES).[54]

Gadolinium complex of 4,7-bis-carboxymethyl-10-[(3,7,12,16,20-pentamethyl-heneicosa-3,7,11,15,19-pentaenylcarbamoyl)-methyl]-1,4,7,10-tetraaza-cyclododec-1-yl}-acetic acid (2). Treatment of the triacid **9b** (0.174 g, 0.23 mmol) with $GdCl_3 \cdot 6H_2O$ according to the general procedure for 60 h at room temperature gave complex **2** as an amorphous powder (0.122 g, 58% yield). The purity of the complex was more than 92% as determined by Evans' method and ICP-AES; IR (neat, cm^{-1}) ν = 2925, 1602, 1384, 1086, 720; MS (ESI^+) m/z (%) = 951.6 (5) $[M+K]^+$, 935.7 (100) $[M+Na]^+$, 919.7 (30) $[M+Li]^+$ displaying the characteristic gadolinium isotopic pattern; HRMS (ESI^+) m/z calc. for $C_{42}H_{69}N_5O_7{}^{158}Gd$ ($[M+H]^+$): 913.4438 Found: 913.4478 (see the ESI†); ICP-AES Calcd. Gd-conc. (found): 1.0 mmol (0.94 mmol).

Gadolinium complex of {4,7-bis-carboxymethyl-10-[(4,8,12,17,21,25-hexamethyl-hexacosa-4,8,12,16,20,24-hexaenylcarbamoyl)-methyl]-1,4,7,10-tetraaza-cyclododec-1-yl}-acetic acid (3). Treatment of the triacid **14b** (0.107 g, 0.13 mmol) with $GdCl_3 \cdot 6H_2O$ according to the general procedure gave complex **3** as an amorphous solid (0.087 g, 68% yield). The purity of the complex was more than 91% as determined by Evans' method and ICP-AES; IR (neat, cm^{-1}) ν = 3389, 3247, 2923, 1602, 1437, 1384, 1319, 1242, 1085, 1003, 904, 840, 802, 721; MS (ESI^-) m/z (%): 993 (100) $[M - H]^-$ displaying the characteristic gadolinium isotopic pattern. HRMS (ESI^-) m/z calc. for $C_{48}H_{77}N_5O_7{}^{158}Gd$, $[M - H]^-$ = 993.4937 Found: 993.4947 (see the ESI†); ICP-AES Calcd. Gd-conc. (found): 1.0 mmol (0.91 mmol).

Gadolinium complex of (4,7-bis-carboxymethyl-10-{[6-(4,8,13,17,21-pentamethyl-docosa-4,8,12,16,20-pentaenoylamino)-hexylcarbamoyl]-methyl}-1,4,7,10-tetraaza-cyclododec-1-yl)-acetic acid (4a). Treatment of the triacid **18b** (0.076 g, 0.086 mmol) with $GdCl_3 \cdot 6H_2O$ according to the general procedure gave complex **4a** as an amorphous solid (0.05 g, 56% yield). The purity of the complex was more than 94% as determined by Evans' method. IR (neat, cm^{-1}) ν = 3396, 3276, 2920, 2855, 1601, 1437, 1384, 1320, 1244, 1084, 1003, 938, 903, 840, 801, 720; MS (ESI^-) m/z (%) = 1038.8 (100) $[M - H]^-$ displaying the characteristic gadolinium isotopic pattern. HRMS (ESI^-) m/z calc. for $C_{49}H_{80}N_6O_8{}^{158}Gd$, $[M - H]^-$: 1038.5243 Found:1038.5279 (see the ESI†).

Gadolinium complex of (4,7-bis-carboxymethyl-10-{[6-(4,8,12,17,21,25-hexamethyl-hexacosa-4,8,12,16,20,24-hexaenoylamino)-hexylcarbamoyl]-methyl}-1,4,7,10tetraaza-cyclododec-1-yl)-acetic acid (4b). Treatment of the triacid **20b** (0.127 g, 0.13 mmol) with $GdCl_3 \cdot 6H_2O$ according to the general procedure gave complex **4b** as an amorphous white solid (0.098 g, 72% yield). The purity of the complex was more than 90% as determined by Evans' method and ICP-AES. IR (neat, cm^{-1}) ν = 3265 (broad), 2923, 2855, 1600, 1435, 1384, 1317, 1242, 1158, 1086, 1003, 937, 904, 839, 802, 714; MS (ESI^-) m/z (%) = 1106.4 (100) $[M - H]^-$ displaying the characteristic gadolinium isotopic pattern. HRMS (ESI^-) m/z calc. for $C_{54}H_{88}N_6O_8{}^{158}Gd$, $[M - H]^-$: 1106.5904 Found:1106.5806 (see the ESI†). ICP-AES Calcd. Gd-conc. (found): 1.0 mmol (0.90 mmol).

Gadolinium complex of [4-({6-[3,5-bis-(4,8,13,17,21-pentamethyl-docosa-4,8,12,16,20-pentaenoylamino)-benzoylamino]-hexylcarbamoyl}-methyl)-7,10-bis-carboxymethyl-1,4,7,10-tetraaza-cyclododec-1-yl]-acetic acid (4c). Treatment of a solution of the triacid **23b** (0.07 g, 0.13 mmol) in ($THF/EtOH/H_2O$, 1/1/1 v/v/v, 14 mL) with $GdCl_3 \cdot 6H_2O$ according to the general procedure gave complex **4c** as an amorphous white solid (0.031 g, 33% overall yield from **23a**) after reverse phase chromatographic purification (MeOH) then ($MeOH/CH_2Cl_2$, 9/1 v/v). The purity of the complex was more than 90% as determined by Evans' method. IR (neat, cm^{-1}) ν = 3600–3200 (broad), 2922, 2855, 1599, 1443, 1383, 1318, 1243, 1086, 1003, 938, 878, 840, 801, 721, 667; MS (ESI^+) m/z (%): = 1595 (35) $[M+K]^+$, 1579 (100) $[M+Na]^+$, 1563 (40) $[M+Li]^+$. MS (ESI^-) m/z (%): = 1555 (100) displaying the characteristic gadolinium isotopic pattern. HRMS (Maldi) m/z calc. for $C_{83}H_{130}N_8O_{10}{}^{158}Gd$, $[M+H]^+$: 1556.9145 Found:1556.9224 (see the ESI†).

Critical micelle concentration (CMC) of SQ-Gd^{3+} complexes using pyrene as a fluorescence probe

Samples for spectroscopic analysis were prepared as follows: a pyrene-saturated solution in MilliQ® water was obtained by stirring overnight a suspension of pyrene in water, followed by filtration to remove excess undissolved pyrene microcrystals. SQ-Gd^{3+} complex (**2–4c** individually) stock solutions (5 g L^{-1}) were prepared in pyrene-saturated water by solubilization (without ethanol or any organic solvent). It was left to equilibrate under agitation over 24 h protected from light at 25 °C. Subsequently, the stock solutions were diluted with pyrene-saturated water to obtain solutions of varying concentrations (1×10^{-4}–1 g L^{-1}), which were further equilibrated under agitation for 24 h. An estimation of the CMC values were obtained by monitoring the changes in the ratio of the pyrene excitation spectra intensities at λ = 333 nm (I_{333}) for pyrene in water and λ = 336 nm (I_{336}) for pyrene in the hydrophobic environment within the micelle core. Excitation spectra were measured at emission wavelength λ_{em} = 390 nm.

Fluorescence spectra were measured at 23 °C with Perkin–Elmer LS-50B (Beaconsfield, Bucks, UK) computer controlled luminescence spectrometer (with FL WinLab software) provided with a thermostated cell.

Nanoassemblies preparation and characterization

Preparation of the NAs of SQ-Gd^{3+} derivatives. All solutions were prepared by weighing. In most cases the samples to be measured were prepared from stock solutions.

(*i*) The micelles were formed spontaneously upon dispersion of the SQ-Gd^{3+} (**2** or **3**) in MilliQ water, (under mechanical stirring; concentrations: 1–10 mg mL^{-1}), and then used without further treatment. (*ii*) The SQ-Gd^{3+} (**4a** and **4b**) were dispersed under mechanical stirring in MilliQ water containing 20% ethanol v/v (concentrations: 1–10 mg mL^{-1}). The solutions were stirred at room temperature until complete dispersion and then the ethanol was evaporated under reduced pressure. (*iii*) The SQ-Gd^{3+} **4c** derivative was solubilized in ethanol 1–10 mg mL^{-1}, then it was nano-precipitated under agitation in 1 mL MilliQ water. Ethanol was then evaporated under reduced pressure at 37.0 ± 0.5 °C using a Buchi Rotavapor® (Switzerland) rotary evaporator.

Preparation of the SQ-gem NAs and their composite NAs with SQ-Gd^{3+} 2

The SQ-gem (alone) nanoassemblies were prepared by nanoprecipitation.[19] Briefly, a solution of SQ-gem in ethanol (1 mL, 2 mg mL^{-1}) was added dropwise under mechanical stirring at room temperature into MilliQ water (1 mL). Then, ethanol was evaporated under reduced pressure.

The composite SQ-gem/SQ-Gd^{3+} **2** nanoassemblies (CNAs) were prepared following similar procedures to SQ-gem by: an ethanolic solution of SQ-gem (0.5 mL, 1 or 2 mg mL^{-1}) was mixed with an ethanolic solution of SQ-Gd^{3+} **2** (0.5 mL. 1 mg mL^{-1}). The resulting mixture (1 mL) was added dropwise under mechanical stirring at room temperature into MilliQ water (1 mL). Ethanol was then evaporated under reduced pressure.

For **FFEM**: more concentrated SQ-gem and SQ-gem/SQ-Gd^{3+} **2** NAs were prepared by the previous described procedures. For SQ-gem alone: a solution (1 mL, 4 mg mL^{-1} ethanol) was nanoprecipited in 1 mL water. For the composite NAs: SQ-gem (4 mg)/SQ-Gd^{3+} **2** (0.5 mg) both in 1 mL ethanol were co-nanoprecipitated, followed by evaporation of the ethanol under reduced pressure, then the weight was adjusted by using milliQ water.

To assess **the amount of SQ-Gd^{3+} 2 incorporated into composites nanoassemblies** (**CNAs**): the CNAs (SQ-gem (1 mg)/SQ-Gd^{3+} **2** (0.5 mg))/1 mL, were centrifuged at 20 °C and 147 000 g (ultracentrifuge Beckmann Coulter LE-80 K, USA) for 60 min. Supernatants were collected, the amount of SQ-Gd^{3+} **2** trapped in the composite nanoparticles was determined as the difference between the total amount of SQ-Gd^{3+} **2** added and the amount of SQ-Gd^{3+} **2** detected in the supernatant by Evans' method. After subtraction the amount of SQ-Gd^{3+} **2** (0.5 mg mL^{-1}) submitted to the same conditions (nanoprecipitation and centrifugation as in the case of CNAs but without SQ-gem), by these procedures it was possible to determine the exact trapped amount of SQ-Gd^{3+}.

Size measurements by dynamic light scattering (DLS)

Nanoassemblies mean size analysis was performed by DLS at a scattering angle of 90° using a Zetasizer Nano ZS (Malvern Instruments, Malvern, UK), provided with a He/Ne laser of 633 nm wavelength. For these measurements, the samples were diluted (1/10) with MilliQ water.

Conventional transmission electron microscopy

Samples for conventional TEM experiments were prepared by depositing 5 µl of the aqueous suspension on 200 mesh copper grids for one minute. Then, a drop of 0.5% aqueous solution of phosphotungstic acid was added on the grid and left for 30 s prior to withdrawal. The remaining liquid was blotted with Whatman filter paper (Whatman International, Maidstone, UK). Observation of the grids was performed on a Philips EM208 electron microscope operating at 80 kV.

Cryogenic transmission electron microscopy (cryo-TEM)

Sample preparation using the cryo-TEM technique was performed as follows: 5 µL of each formulation was placed on 300 mesh Lacey Formvar/Carbon coated copper grids (Ted Pella Inc. Redding, CA). The excess amount of liquid was then blotted with a Whatman No.5 filter paper, and the grids were immediately plunged into a liquid ethane bath cooled with liquid nitrogen using a Leica EM CPC Cryo-workstation (Leica Microsystems SAS, Rueil Malmaison, France). Afterward, the grids were constantly maintained in liquid nitrogen and carefully transferred in a cryo-holder (626 DH Gatan). Preparations were investigated at –170 °C on a cryo-TEM (JEOL 2100) electron microscope operating at an accelerating voltage of 200 kV under low electron dose.

Electron microscopy after freeze-fracture (FFEM)

The nanoassemblies, previously incubated with glycerol (30% v/v) used as a cryoprotectant, were visualised by TEM after freeze-fracture. Briefly, a drop of each sample was placed on a copper support and immediately frozen in liquid propane cooled with liquid nitrogen, and then kept in liquid nitrogen. Fracturing and shadowing were performed in a BAL-TEC BAF 060 – Freeze Fracture & Freeze Etching System. The replicas were washed in THF and distilled water and placed on copper grids. Observations were made under a transmission electron microscope Philips CM120 operating at 120 kV.

Characterization by X-ray diffraction (XRD)

The structure of **4c** was further investigated by small-angle X-ray scattering (SAXS).

Experiments were performed on the SWING synchrotron beamline at Synchrotron SOLEIL (http://www.synchrotron-soleil.fr/Recherche/LignesLumiere/SWING) operated at 12 keV. The sample was loaded in a quartz capillary (1.5 mm diameter, GLASS W. Müller, Berlin, Germany). The X-ray pattern was recorded at 20 °C by a two-dimensional CCD detector. The scattered intensity was reported as a function of the scattering vector (q)

$$q = 4\pi\sin\theta/\lambda \quad (1)$$

where 2θ is the scattering angle and λ the wavelength.

The calibration of the q-range was carried out with the 2Lβ form of pure tristearin (d-spacing 44.97 ± 0.05 Å),[55] and silver behenate (d-spacing 58.38 ± 0.01 Å).[56]

Concentrations

All gadolinium concentrations were determined by Evans' method[53] (see the ESI†) and by inductively coupled plasma atomic emission spectroscopy ICP-AES.

Proton relaxation rate analysis of the SQ-Gd^{3+} complexes

For T_1 measurements at fixed magnetic fields, the standard inversion-recovery method was used as the pulse sequence. The longitudinal relaxivities r_1 were then determined from the slope of the linear regressions fits of $1/T_1$ *versus* the SQ-Gd^{3+} concentrations. Proton nuclear magnetic relaxation dispersion (NMRD) profiles were obtained at 310 K on a field cycling relaxometer (Stelar, Mede, Italy). The range of magnetic fields covered varied from 0.47 mT to 0.24 T, which corresponded to frequencies varying from 0.02 to 10 MHz. Additional longitudinal and transverse relaxation rates were measured on Bruker Minispecs mq20 (20 MHz, 0.47 T), mq60 (60 MHz, 1.41 T) (Bruker, Karlsruhe, Germany), and Bruker Avance 400 (400 MHz, 9.4 T). T_1 relaxation times were recorded in MilliQ water, or a solution of freshly prepared 4% HSA in MilliQ water, in the concentration ranges 0.1–2 mM of SQ-Gd^{3+}. The T_1 relaxivity (r_1) of SQ-Gd^{3+} complex was obtained by the relationship given in eqn (2),

$$r_1 = \frac{R_1^{obs} - R_1^{m}}{C} \quad (2)$$

Where $R_1{}^{obs}$, $R_1{}^{m}$ are the relaxation rates $1/T_1$ (s^{-1}) of the sample and the matrix respectively (matrix = the system before addition of the CA: water alone or HSA 4% in water), and C is the concentration of the paramagnetic SQ-Gd^{3+} complex (mM). The $R_1{}^{obs}$ values of each dilution were plotted against the Gd^{3+} concentration to give the concentration dependent relaxation rate relationship. Proton NMRD curves were fitted using data processing software including different theoretical models describing nuclear relaxation phenomena (Minuit, CERN Library).[57–61]

Variable temperature ^{17}O measurements

For ^{17}O measurements, an aqueous solution containing 2.6% ^{17}O isotope (WATER (17O, 35–40%), Cambridge Isotope Laboratories, Inc. MA, USA) was used. Variable temperature ^{17}O NMR measurements were recorded at 400 MHz (9.4 T; 54.2 MHz) on a Bruker Avance spectrometer, equipped with a 5 mm probe, by using a D_2O external lock. Experimental settings were as follows: spectral width of 10.000 Hz, 90° pulse for 14 μs, acquisition time 10 ms, 1024 scans and without sample spinning. The observed transverse relaxation rates $R_2{}^{obs}$ were calculated from the signal width at half-height ($\Delta\nu_{1/2}$): $R_2{}^{obs} = \pi\Delta\nu_{1/2}$.

Cytotoxicity assay on MIA PaCa-2 cells

Human pancreatic cancer cells (MIA PaCa-2) were cultured in DMEM (Dulbecco's Modified Eagle Medium) supplemented with 10% fetal calf serum, 2.5% horse serum, 50 U mL^{-1} penicillin and 50 μg mL^{-1} streptomycin and 2 mM L-glutamine. The anticancer activity of gemcitabine (1 mg mL^{-1}), SQ-gem (1 mg mL^{-1}), and SQ-gem/SQ-Gd^{3+} **2** (1 mg/0.5 mg mL respectively) towards this cell line was determined using the 3-[4, 5-dimethylthiazol-2-yl]-3,5-diphenyl tetrazolium bromide (MTT) test, measuring mitochondrial dehydrogenase activity. The cells in exponential growth phase were seeded into 96-well plates and were pre-incubated for 24 h at 37.0 ± 0.5 °C in a humidified atmosphere of 5% CO_2 in air. Different dilutions of gemcitabine, SQ-gem, and the SQ-gem/SQGd^{3+} **2** were added to the cells in the culture medium. Each dilution was tested in triplicate. After 72 h at 37.0 ± 0.5 °C, 200 μL of MTT solution in cell culture medium (0.5 mg mL^{-1}) were added to each well. After incubation for 2.5 h at 37.0 ± 0.5 °C, the culture medium was removed and the resultant formazan crystals were dissolved in 200 μL dimethylsulfoxide. The absorbance of converted dye, which is proportional to the number of viable cells, was measured at 570 nm using a microplate reader (Metertech Σ 960, Fisher Bioblock, France). The percentage of surviving cells was calculated as the absorbance ratio of treated to untreated cells.

Acknowledgements

The authors thank Corinne Pierart (Univ. Mons, B-7000 Mons, Belgium) for her help in relaxometric evaluation of the SQ-Gd^{3+} complexes, Michèle Danet (CNRS 8076 BIOCIS, France) is warmly acknowledged for performing mass spectra. Damascus University, Damascus, Syria is acknowledged for its financial support to Mohammad Othman. The research leading to these results has received funding from the European Research Council under the European Community's Seventh Framework Programme FP7/2007-2013 Grant Agreement no.249835, and ANR: Agence Nationale de la Recherche, France.

References

1 R. J. M. van Geuns, H. G. de Bruin, B. J. W. M. Rensing, P. A. Wielopolski, M. D. Hulshoff, P. M. A. van Ooijen, M. Oudkerk and P. J. de Feyter, *Heart*, 1999, **82**, 515–519.
2 P. Caravan, J. J. Ellison, T. J. McMurry and R. B. Lauffer, *Chem. Rev.*, 1999, **99**, 2293–2352.
3 M. Holz, *Magn. Reson. Chem.*, 1993, **31**, S154.
4 S. Aime, M. Botta, M. Fasano and E. Terreno, *Chem. Soc. Rev.*, 1998, **27**, 19–29.
5 S. Aime, D. D. Castelli, S. G. Crich, E. Gianolio and E. Terreno, *Acc. Chem. Res.*, 2009, **42**, 822–831.
6 S. Aime and P. Caravan, *J. Magn. Reson. Imaging*, 2009, **30**, 1259–1267.
7 D. Parker, R. S. Dickins, H. Puschmann, C. Crossland and J. A. K. Howard, *Chem. Rev.*, 2002, **102**, 1977–2010.
8 A. E. Merbach and É. Tóth, *The Chemistry of Contrast Agents in Medical Magnetic Resonance Imaging*, (ed.: É. Tóth and A. E. Merbach) Wiley and Sons, New York, 2001.
9 E. Toth, L. Helm and A. E. Merbach, in *The chemistry of contrast agents in medical magnetic resonance imaging*, (ed.: É. Tóth and A. E. Merbach) Wiley and Sons, New York, 2001, pp. 45–119.
10 S. Aime, I. M. Botta, F. Fedeli, E. Gianolio, E. Terreno and P. Anelli, *Chem.–Eur. J.*, 2001, **7**, 5261–5269.
11 P. Caravan, *Acc. Chem. Res.*, 2009, **42**, 851–862.
12 P. Caravan, *Chem. Soc. Rev.*, 2006, **35**, 512–523.
13 A. Accardo, D. Tesauro, L. Aloj, C. Pedone and G. Morelli, *Coord. Chem. Rev.*, 2009, **253**, 2193–2213.
14 W. J. M. Mulder, G. J. Strijkers, G. A. F. van Tilborg, D. P. Cormode, Z. A. Fayad and K. Nicolay, *Acc. Chem. Res.*, 2009, **42**, 904–914.
15 W. J. M. Mulder, G. J. Strijkers, G. A. F. van Tilborg, A. W. Griffioen and K. Nicolay, *NMR Biomed.*, 2006, **19**, 142–164.
16 E. Battistini, E. Gianolio, R. Gref, P. Couvreur, S. Fuzerova, M. Othman, S. Aime, B. Badet and P. Durand, *Chem.–Eur. J.*, 2008, **14**, 4551–4561.
17 Y. Matsumura and H. Maeda, *Cancer Research*, 1986, **46**, 6387–6392.
18 A. M. Morawski, G. A. Lanza and S. A. Wickline, *Curr. Opin. Biotechnol.*, 2005, **16**, 89–92.

19 P. Couvreur, B. Stella, L. H. Reddy, H. Hillaireau, C. Dubernet, D. Desmaele, S. Lepetre-Mouelhi, F. Rocco, N. Dereuddre-Bosquet, P. Clayette, V. Rosilio, V. Marsaud, J. M. Renoir and L. Cattel, *Nano Lett.*, 2006, **6**, 2544–2548.
20 P. Couvreur, L. H. Reddy, S. Mangenot, J. H. Poupaert, D. Desmaele, S. Lepetre-Mouelhi, B. Pili, C. Bourgaux, H. Amenitsch and M. Ollivon, *Small*, 2008, **4**, 247–253.
21 F. Bekkara-Aounallah, R. Gref, M. Othman, L. H. Reddy, B. Pili, V. Allain, C. Bourgaux, H. Hillaireau, S. Lepêtre-Mouelhi, D. Desmaële, J. Nicolas, N. Chafi and P. Couvreur, *Adv. Funct. Mater.*, 2008, **18**, 3715–3725.
22 E. E. van Tamelen and T. J. Curphey, *Tetrahedron Lett.*, 1962, **3**, 121–124.
23 P. A. S. Smith, *Org. React.*, 1946, **3**, 337–449.
24 I. Mamedov, A. Mishra, G. Angelovski, H. A. Mayer, L. O. Palsson, D. Parker and N. K. Logothetis, *Dalton Trans.*, 2007, 5260–5267.
25 A. Barge, G. Cravotto, E. Gianolio and F. Fedeli, *Contrast Media Mol. Imaging*, 2006, **1**, 184–188.
26 E. H. Eschinasi, *J. Org. Chem.*, 1970, **35**, 1598–1600.
27 W. S. Johnson, L. Werthemann, W. R. Bartlett, T. J. Brocksom, T.-T. Li, D. J. Faulkner and M. R. Petersen, *J. Am. Chem. Soc.*, 1970, **92**, 741–743.
28 M. S. Gibson and R. W. Bradshaw, *Angew. Chem., Int. Ed. Engl.*, 1968, **7**, 919–930.
29 J. Mulzer, A. Angermann, B. Schubert and C. Seilz, *J. Org. Chem.*, 1986, **51**, 5294–5299.
30 P. Singh, *Bioconjugate Chem.*, 1998, **9**, 54–63.
31 J. Sam, W. F. Minor and Y. G. Perron, *J. Am. Chem. Soc.*, 1959, **81**, 710–713.
32 M. Wilhelm, C. L. Zhao, Y. Wang, R. Xu, M. A. Winnik, J. L. Mura, G. Riess and M. D. Croucher, *Macromolecules*, 1991, **24**, 1033–1040.
33 M. F. Francis, L. Lavoie, F. M. Winnik and J. C. Leroux, *Eur. J. Pharm. Biopharm.*, 2003, **56**, 337–346.
34 G. M. Nicolle, É. Tóth, K.-P. Eisenwiener, H. R. Mäcke and A. E. Merbach, *JBIC, J. Biol. Inorg. Chem.*, 2002, **7**, 757–769.
35 A. Accardo, D. Tesauro, G. Morelli, E. Gianolio, S. Aime, M. Vaccaro, G. Mangiapia, L. Paduano and K. Schillen, *JBIC, J. Biol. Inorg. Chem.*, 2007, **12**, 267–276.
36 P. Winter, P. Athey, G. Kiefer, G. Gulyas, K. Frank, R. Fuhrhop, D. Robertson, S. Wickline and G. Lanza, *J. Magn. Magn. Mater.*, 2005, **293**, 540–545.
37 G. Liu, C. E. Conn, L. J. Waddington, S. T. Mudie and C. J. Drummond, *Langmuir*, 2009, **26**, 2383–2391.
38 M. Oliver, A. Ahmad, N. Kamaly, E. Perouzel, A. Caussin, M. Keller, A. Herlihy, J. Bell, A. D. Miller and M. R. Jorgensen, *Org. Biomol. Chem.*, 2006, **4**, 3489–3497.
39 C. Czeslik, O. Reis, R. Winter and G. Rapp, *Chem. Phys. Lipids*, 1998, **91**, 135–144.
40 S. Hak, H. M. Sanders, P. Agrawal, S. Langereis, H. Grull, H. M. Keizer, F. Arena, E. Terreno, G. J. Strijkers and K. Nicolay, *Eur. J. Pharm. Biopharm.*, 2009, **72**, 397–404.
41 S. Laurent, L. V. Elst and R. N. Muller, *Contrast Media Mol. Imaging*, 2006, **1**, 128–137.
42 S. Laurent, L. Vander Elst, C. Thirifays and R. Muller, *Eur. Biophys. J.*, 2008, **37**, 1007–1014.
43 V. C. Pierre, M. Botta and K. N. Raymond, *J. Am. Chem. Soc.*, 2004, **127**, 504–505.
44 M. V. Rekharsky and Y. Inoue, *Chem. Rev.*, 1998, **98**, 1875–1918.
45 G. J. Strijkers, W. J. M. Mulder, R. B. van Heeswijk, P. M. Frederik, P. Bomans, P. C. M. M. Magusin and K. Nicolay, *MAGMA. Magn. Reson. Mater. Phys. Biol. Med.*, 2005, **18**, 186–192.
46 M. Oliver, A. Ahmad, N. Kamaly, E. Perouzel, A. Caussin, M. Keller, A. Herlihy, J. Bell, A. D. Miller and M. R. Jorgensen, *Org. Biomol. Chem.*, 2006, **4**, 3489–3497.
47 J. Theodore Peters, *All About Albumin Biochemistry, Genetics and Medical Applications* Academic Press, New York, 1996.
48 C. Henoumont, L. Vander Elst, S. Laurent and R. Muller, *JBIC, J. Biol. Inorg. Chem.*, 2009, **14**, 683–691.
49 P. Caravan, N. J. Cloutier, M. T. Greenfield, S. A. McDermid, S. U. Dunham, J. W. Bulte, J. C. Amedio, Jr., R. J. Looby, R. M. Supkowski, W. D. Horrocks, Jr., T. J. McMurry and R. B. Lauffer, *J. Am. Chem. Soc.*, 2002, **124**, 3152–3162.
50 R. B. Lauffer, D. J. Parmelee, S. U. Dunham, H. S. Ouellet, R. P. Dolan, S. Witte, T. J. McMurry and R. C. Walovitch, *Radiology*, 1998, **207**, 529–538.
51 J. M. Seddon, J. Robins, T. Gulik-Krzywicki and H. Delacroix, *Phys. Chem. Chem. Phys.*, 2000, **2**, 4485–4493.
52 G. C. Shearman, B. J. Khoo, M.-L. Motherwell, K. A. Brakke, O. Ces, C. E. Conn, J. M. Seddon and R. H. Templer, *Langmuir*, 2007, **23**, 7276–7285.
53 D. M. Corsi, C. Platas-Iglesias, H. v. Bekkum and J. A. Peters, *Magn. Reson. Chem.*, 2001, **39**, 723–726.
54 C. Gløgård, R. Hovland, S. L. Fossheim, A. J. Aasen and J. Klaveness, *J. Chem. Soc., Perkin Trans. 2*, 2000, 1047–1052.
55 F. Lavigne, C. Bourgaux and M. Ollivon, *J. Phys.*, 1993, **4**, 137–138.
56 T. C. Huang, H. Toraya, T. N. Blanton and Y. Wu, *J. Appl. Crystallogr.*, 1993, **26**, 180–184.
57 I. Solomon, *Phys. Rev.*, 1955, **99**, 559–565.
58 N. Bloembergen, *J. Chem. Phys.*, 1957, **27**, 572–573.
59 J. H. Freed, *J. Chem. Phys.*, 1978, **68**, 4034–4037.
60 R. N. Muller, D. Declercq, P. Vallet, F. Giberto, B. Daminet, H. W. Fischer, F. Maton and V. Haverbeke, in *'Proc. ESMRMB, 7th Annual Congress' Strasbourg*, 1990, vol. 394.
61 P. Vallet, *Relaxivity of nitroxide stable free radicals. Evaluation by field cycling method and optimisation*, PhD Thesis, University of Mons-Hainaut, Belgium, 1992.

